ELSEVIER

Journal of Magnetism and Magnetic Materials 192 (1999) 203–232

Journal of magnetism and magnetic materials

Exchange bias

J. Nogués[a], Ivan K. Schuller[b,*]

[a] *Grup d'Electromagnetisme, Department de Física, Universitat Autònoma de Barcelona, 08193 Bellaterra, Spain*
[b] *Physics Department 0319, University of California – San Diego, La Jolla, CA 92093-0319, USA*

Received 5 March 1998; received in revised form 7 July 1998

Abstract

We review the phenomenology of exchange bias and related effects, with emphasis on layered antiferromagnetic (AFM)–ferromagnetic (FM) structures. A compilation of materials exhibiting exchange bias and some of the techniques used to study them is given. Some of the applications of exchange bias are discussed. The leading theoretical models are summarized. Finally some of the factors controlling exchange bias as well as some of the unsolved issues associated with exchange bias are discussed.

PACS: 75.50.Rr; 75.70.Cn; 75.70. − i; 75.30.Gw

Keywords: Exchange bias; Interfaces; Ferromagnetism; Antiferromagnetism

1. Introduction

When materials with ferromagnetic (FM)–antiferromagnetic (AFM) interfaces are cooled through the Néel temperature (T_N) of the AFM (with the Curie temperature, T_C of the FM larger than T_N) an anisotropy ('exchange bias') is induced in the FM [1–10]. Exchange bias is one of the phenomena associated with the exchange anisotropy created at the interface between an AFM and an FM material.

This anisotropy was discovered in 1956 by Meiklejohn and Bean when studying Co particles embedded in their native antiferromagnetic oxide (CoO) [11]. Since then it was observed in many different systems containing FM–AFM interfaces, such as small particles (Section 3.1) [1–7,9], inhomogeneous materials (Section 3.2) [1,2,7–10], FM films on AFM single crystals (Section 3.3) [12,13] and thin films (Section 3.4) [2,9,14–16]. In this review we will focus mainly on layered AFM–FM. Thin AFM–FM bilayers are favored because of the improved control over the interface and because they are more amenable for the development of devices [17,18]. In addition to AFM–FM interfaces, exchange bias and related effects have also been observed in other types of interfaces, e.g. involving ferrimagnets (ferri): AFM–ferri [19], ferri–FM [20].

Possible applications of these effects include permanent magnets [6], magnetic recording media

* Corresponding author. Tel.: + 1 619 5342450; fax: + 1 619 5340173; e-mail: ischuller@ucsd.edu.

0304-8853/99/$ – see front matter
PII: S0304-8853(98)00266-2

[21,22] or domain stabilizers in recording heads based on anisotropic magnetoresistance [18]. However, it was the reduction of the saturation fields to observe giant magnetoresistance (GMR) in exchange biased systems [23], as compared to standard GMR multilayer systems [24], which triggered a renewed interest in these phenomena [17].

1.1. Phenomenology

Interface coupling due to exchange anisotropy is observed cooling the AFM–FM couple in the presence of a static magnetic field from a temperature above T_N, but below T_C ($T_N < T < T_C$) to temperatures $T < T_N$ [1–10]. The hysteresis loop of the AFM–FM system at $T < T_N$ after the field cool procedure, is shifted along the field axis generally in the opposite ('negative') direction to the cooling field (see Fig. 1), i.e. the absolute value of coercive field for decreasing and increasing field is different. This loop shift is generally known as *exchange bias*, H_E. The hysteresis loops also have an increased coercivity, H_C, after the field cool procedure. Both these effects disappear at, or close to, the AFM Néel temperature confirming that it is the presence of the AFM material which causes this anisotropy [1–10].

Torque magnetometry at $T < T_N$ after field cool, shows an additional sin ϕ component to the torque magnetization, where ϕ is the angle between the applied field and the cooling field direction. Fig. 2a shows the combination of a $\sin^2\phi$ (uniaxial anisotropy) component with a sin ϕ component for an oxidized Co layer. A purely uniaxial torque ($\sin^2\phi$) has two minima 180° apart, however in AFM–FM systems, due to the presence of the sin ϕ component, the torque magnetization has only one absolute minimum. In other words, instead of uniaxial anisotropy, i.e. two equivalent easy configurations in opposite directions, the magnetization in AFM–FM systems has only one easy direction, often denoted as *unidirectional anisotropy*. As shown in Fig. 2a the clockwise and counterclockwise torques are different. The area between both torque curves gives twice the energy lost in rotating the magnetization, denoted as rotational hysteresis. This type of hysteresis is present in FM systems only in a narrow field range, however, AFM–FM

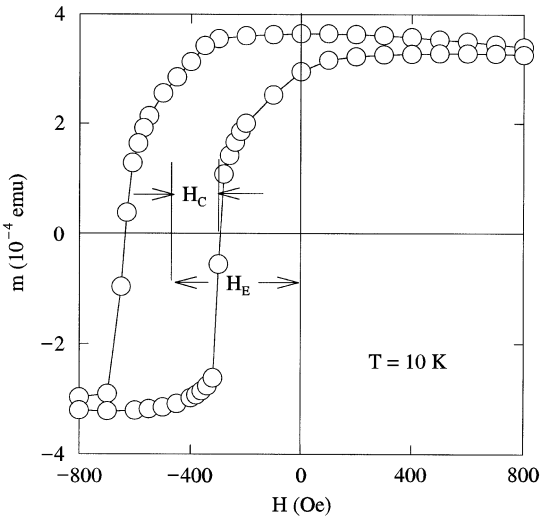

Fig. 1. Hysteresis loop, $m(H)$, of a FeF_2/Fe bilayer at $T = 10$ K after field cooling [72]. The exchange bias, H_E, and the coercivity, H_C, are indicated in the figure.

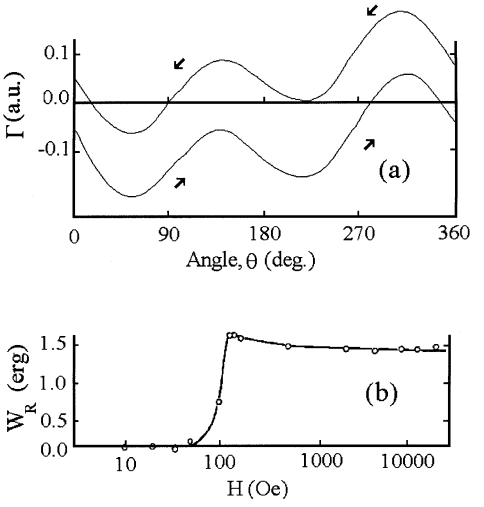

Fig. 2. (a) Torque magnetization, Γ, and (b) rotational hysteresis, W_R for an oxidized Co film at $T = 77$ K after field cooling [16].

systems have a non-vanishing rotational hysteresis even at high fields (Fig. 2b). The unidirectional anisotropy and the non-vanishing rotational hysteresis also disappear at, or below, T_N [1–3,5–9].

Finally, it is noteworthy that the above effects are not present (or are reduced) if the AFM–FM couple

is cooled in zero field from a demagnetized state [1–10]. However, exchange bias properties are still present if the AFM–FM system is zero field cooled from a remanent state [25].

1.2. Intuitive picture

Unidirectional anisotropy and exchange bias can be qualitatively understood by assuming an exchange interaction at the AFM–FM interface [1,3]. When a field is applied in the temperature range $T_N < T < T_C$, the FM spins line up with the field, while the AFM spins remain random (Fig. 3a(i)). When cooling to $T < T_N$, in the presence of the field, due to the interaction at the interface, the AFM spins next to the FM align ferromagnetically to those of the FM (assuming ferromagnetic interaction). The other spin planes in the AFM "follow" the AFM order so as to produce zero net magnetization (Fig. 3a(ii)). When the field is reversed, the FM spins start to rotate. However, for sufficiently large AFM anisotropy, the AFM spins remain unchanged (Fig. 3a(iii)). Therefore, the interfacial interaction between the FM–AFM spins at the interface, tries to align ferromagnetically the FM spins with the AFM spins at the interface. In other words, the AFM spins at the interface exert a microscopic torque on the FM spins, to keep them in their original position (ferromagnetically aligned at the interface) (Fig. 3a(iii)). Therefore, the FM spins have one single stable configuration, i.e. the anisotropy is *unidirectional*. Thus, the field needed to reverse completely an FM layer will be larger if it is in contact with an AFM, because an extra field is needed to overcome the microscopic torque (Fig. 3b). However, once the field is rotated back to its original direction, the FM spins will start to rotate at a smaller field, due to the interaction with the AFM spins (which now exert a torque in the same direction as the field) (Fig. 3a(v) and Fig. 3b). The material behaves as if there was an extra (internal) biasing field, therefore, the FM hysteresis loop is shifted in the field axis, i.e. *exchange bias* [1–3,7,9].

Although this simple phenomenological model gives an intuitive picture, there is little quantitative understanding of these phenomena. Moreover, the role of the many different parameters involved in exchange bias, such as anisotropy, roughness, spin configuration or magnetic domains, is far from being understood. Finally, a clear understanding of exchange bias at the microscopic level is still lacking.

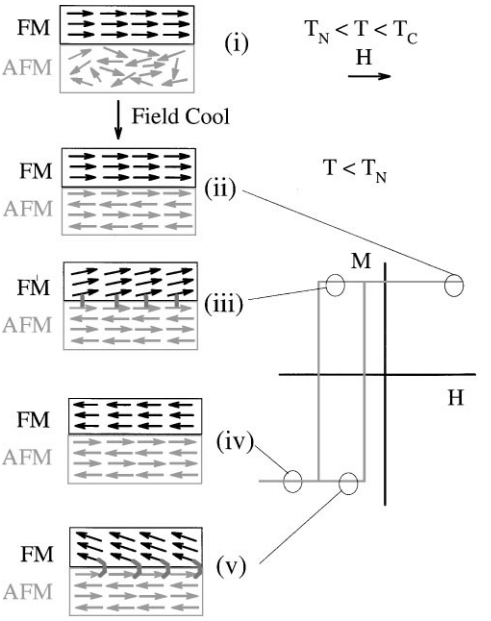

Fig. 3. Schematic diagram of the spin configuration of an FM–AFM bilayer (a) at different stages (i)–(v) of an exchange biased hysteresis loop (b). Note that the spin configurations are just a simple cartoon to illustrate the effect of the coupling and they are not necessarily accurate portraits of the actual rotation of the FM or AFM magnetizations.

In this review we will discuss the present status of this field. We will present the most common techniques (Section 2), the materials involved (Section 3), some applications (Section 4), theoretical aspects (Section 5) and several interesting open issues (Section 6).

2. Techniques

Exchange bias and related effects have been investigated using many experimental techniques. The most commonly used techniques and the main information they provide are summarized below.

2.1. Magnetization

Hysteresis loops, obtained from magnetization versus applied field, is the most commonly used technique to study exchange bias materials. Hysteresis loops have been measured using a wide variety of instruments [3,11,16,21,26–60], most commonly SQUID [12,19,25,61–109], vibrating sample magnetometer (VSM) [61,70,84–86,88–90,99,100,104, 107,108,110–185], Kerr effect [15,20,120,186–215] and loop tracers [84,114,122,143,161,162,176,190, 197,198,211,212,215–227]. The main information obtained from these techniques is the loop shift, H_E, and coercivity, H_C (see Fig. 1), although some information about anisotropies can also be obtained from the shape of the hysteresis loops.

It is noteworthy that from hysteresis loops and other DC-experiments (e.g. torque), only the lower limit of the interface AFM–FM coupling is obtained [228]. However, larger values are obtained from certain AC-measurements which relay on small oscillations of the FM magnetization from its remanent or saturated state, such as magnetoresistance [229,230], AC-susceptibility [231] or Brillouin light scattering [232].

2.2. Torque

Torque magnetometer, in which the magnetization is measured while rotating the sample in a field, gives information about the anisotropies present. It is the presence of a $\sin\phi$ component in the torque (Fig. 2a) which confirms the unidirectionality of the anisotropy [3,11,13,16,27,28,33, 34,131,137,186,190,191,203,212,216,233–242]. Moreover, torque magnetometry can reveal an additional sign of exchange anisotropy, i.e. the presence of high field rotational hysteresis [3,11,13,16, 27,28,34,131,186,190,191,203,212,233,234,236,237, 239–243] (Fig. 2b).

2.3. Ferromagnetic resonance

In ferromagnetic resonance (FMR) the samples mounted in a microwave cavity are subject to a high frequency (GHz) magnetic field while a DC field is swept through resonance. From the resonance positions and line shapes it is possible to extract the exchange bias and anisotropies [121, 148,174,244–260]. Under certain conditions, spin wave resonances (SWR) are observed in AFM–FM bilayers [244,246,252–254,256–260], from the position of the SWR the FM stiffness, A_{FM}, is obtained.

Most FMR measurements imply that the magnetization of the FM layer is not homogeneous throughout the thickness of the layer, i.e. although the spins on the top of the FM layer are aligned with the field, the spins close to the interface may have other orientations (denoted as transition layer) [249–251,254,255,257,258].

2.4. Neutron diffraction

Due to the magnetic nature of the neutrons, neutron diffraction is the ideal probe for the magnetic structure in addition to the physical structure.

Grazing incidence neutron diffraction, determines the homogeneity of the FM and AFM layers (formation of domains), by probing the magnetization as a function of the depth with a 1–2 nm resolution [97,98,261–267]. Contrary to what is observed by other techniques, FM–AFM systems do not appear to form domains in the FM or AFM layers, however, measurements in ferri–AFM multilayers indicate that the ferrimagnetic layer is not homogeneous throughout its thickness [266,267]. To enhance the diffraction signal in neutron diffraction often multilayers of the type $n\times$[ferri–AFM] or [FM–AFM] are investigated [97,98,101,265–270]. It is noteworthy that from grazing angle studies the hysteresis loops, and thus H_E and H_C, can be extracted by calculating the polarization function for different applied fields [261,262].

High angle neutron diffraction has also been applied to the study of exchange bias [97,98, 101,268,269]. The main information obtained from this method is the spin configuration of the different magnetic layers. However, other types of information such as domain formation can be extracted indirectly (e.g. peak widths) from the scans. An important result obtained from high angle neutron diffraction on Fe_3O_4/NiO and Fe_3O_4/CoO multilayers is the possible presence of domains in the AFM NiO [269] or CoO [101]

layers and a perpendicular (i.e. non-collinear) coupling between the AFM and ferri spins at the interface [101].

2.5. Magnetoresistance

The measurement of the field dependence of the resistivity, the magnetoresistance, has been used in two different ways to explore exchange bias. Information about exchange bias can be obtained from 'spin valve' devices (AFM–FM–non-magnetic–FM) [23,41,47,75,81–83,106,124,128,132,133,149–154,156,157,168,177–180,183,194,199,225,271–293]. The full magnetoresistance curve (i.e. measured to saturation of both FM layers) provides both H_E and H_C of an AFM–FM couple as shown in Fig. 4 (see Section 4 for more details). Magnetoresistance measurements of simple AFM–FM bilayers have been used to determine H_E, H_C or anisotropy constants [58,229,230,294–297].

An important result from some of these studies is the indication that the FM layer appears to form a transition layer at the interface [229,230,294–297].

2.6. AC-susceptibility

In AC-susceptibility, the change in magnetic flux created by the sample due to the presence of an alternating field is measured as a function of the applied AC and DC fields, temperature or frequency. H_E and H_C are obtained from the DC field dependence of the AC-susceptibility. High frequency, $H_{DC} = 0$ [248], $H_{DC} \neq 0$ [298], low frequency $H_{DC} \neq 0$ [231], and critical curve measurements [58,299] susceptibility measurements have been carried out in FM–AFM bilayers.

The results from AC-susceptibility also seem to indicate that the FM layer appears not to be homogeneous throughout its thickness [231,248,298].

2.7. Domain observation

FM and AFM domains could have an important effect on H_E. Thus FM domain formation has been studied using several techniques, such as Bitter method [137,203,204,300], Kerr effect [16,20,204,205,301], Lorentz microscopy [281,302–304],

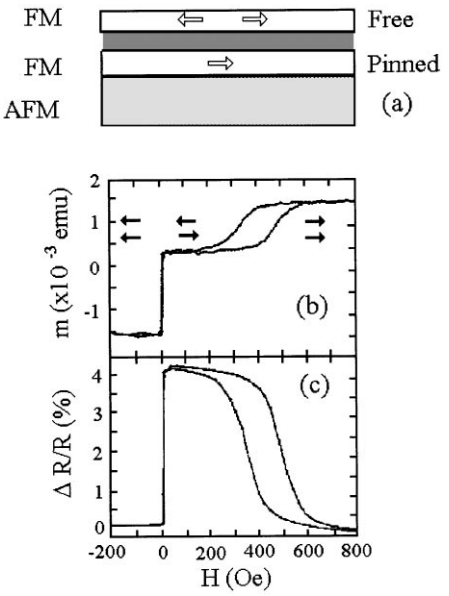

Fig. 4. (a) Schematic diagram of a spin valve device. (b) Hysteresis loop, $m(H)$, and (c) magnetoresistance, $\Delta R/R(H)$, of $Fe_{20}Ni_{80}/Cu/Fe_{20}Ni_{80}/FeMn$ GMR spin valve at room temperature [23].

Faraday effect [305], interface colloidal contrast [306], spin polarized secondary electron microscopy [307] or magnetic force microscopy (MFM) [181,182,308]. These techniques allow only studies of the surface FM domain formation (perpendicular to the interface), i.e. domains parallel to the interface (predicted indirectly by several other techniques [229–231,248–251,255,257,258,266,267,294,296–298]) cannot be observed. However, in some cases changes in the local anisotropy due to the presence of the AFM can be detected [303,304,307].

The detailed behavior of the FM domains depends on the AFM–FM system studied and the thickness of the FM film, probably due to the different anisotropies of the AFM and/or FM materials. Due to the hysteresis loop shift, the domain structure always appears at higher fields than for single FM layers. Usually the domain structure in AFM–FM bilayers is more 'complicated' (i.e. more sizes, shapes and types of domains) than for single FM films. The size and morphology of the domains is also system dependent [16,20,137,181,182,203–205,281,300–308]. From these domain

observations indirect values of H_E and H_C are obtained by analyzing the area of opposite domains (parallel and antiparallel with the field) for different applied fields [181,182].

2.8. Brillouin scattering

In Brillouin scattering the samples are irradiated with a laser beam, in the visible range, and the scattered light is measured as a function of scattering geometry, field and temperature. The changes in the scattered spectrum together with the scattering geometry give information on the spin waves frequency. From the shift of the spin wave frequency, exchange bias H_E is obtained in the saturated state [232,309]. Results in Fe/FeF_2 bilayers indicate inhomogeneities in the FM layer below T_N [232].

2.9. Magnetic dichroism

In this technique, the electrons in the sample are excited with X-rays, and the photon energy emitted by the electrons recombining to the ground state is measured as a function of the magnetic field and temperature. The high sensitivity to different elements, allows material specific properties to be studied independently. Moreover, magnetic dichroism can probe the magnetic properties at different depths, allowing the study of buried layers or interfaces [310].

2.10. Mössbauer effect

If in the AFM and/or FM layer a radioactive isotope of one of the materials composing the AFM or FM layer is introduced, the Mössbauer effect can be studied. In this technique, the γ-rays emitted by the radioactive isotopes are measured. This technique is very sensitive to the local atomic configuration, thus if the radioactive isotopes are placed at a certain position in the material (surface, bulk, interface), information about the local configuration in that specific area can be obtained by comparing the spectra of the radioactive atoms in different positions [167,209,311]. Results in $FeMn/Fe_{20}Ni_{80}$ indicate that interface and bulk atoms behave in a similar fashion [209].

3. Materials

3.1. Small particles

Fine particles were the first type of system where exchange bias was observed. Since its discovery, exchange bias in small particles has been observed in a number of materials, mainly ferromagnetic particles covered with their antiferromagnetic or ferrimagnetic native oxide: Co–CoO [3,11,26,61–64], Ni–NiO [5,26,65,107,108], Fe–FeO [243], FeCo–FeCoO [27], Fe–Fe_3O_4 [65,66,110] (Table 1). However, other combinations of materials have also been studied, such as nitrides Fe–Fe_2N [110], Co–CoN [61] or sulfides Fe–FeS [26,233,234] (Table 1). The particles studied are usually in the nanometer range (10–100 nm) and produced by a variety of methods, such as electrodeposition, vapor deposition, gas condensation, reduction of the oxalate or mechanical alloying.

A general trend exhibited by most fine particles systems is the existence of non-vanishing rotational hysteresis [3,5,11,26,61–64,233,234,243] and an increase of coercivity below T_N [3,11,26,61–66,107,108,110,233,234]. However, only for Co–CoO,

Table 1
Summary of exchange bias and related properties for different small particle systems. Note that the given loop shifts, H_E, are at $T = 4$–10 K

Material	H_E	H_C enhancement	Rotational hysteresis
Co–CoO[c]	Large (9500 Oe)[a]	Yes	Yes
Co–CoN[d]	Large (3200 Oe)	Yes	–[b]
Ni–NiO[e]	Small (400 Oe)	Yes	Yes
Fe–FeO[f]	None	–	Yes
Fe–Fe_3O_4[g]	Small (120 Oe)	Yes	–
Fe–FeS[h]	–	Yes	Yes
Fe–Fe_2N[i]	Small (300 Oe)	Yes	–

[a]Given in brackets is the maximum reported H_E.
[b]Dashes indicate that this property has not been studied in the system.
[c][3,11,26,61–64].
[d][61].
[e][5,26,65,107,108].
[f][243].
[g][65,66,110].
[h][26,233,234].
[i][110].

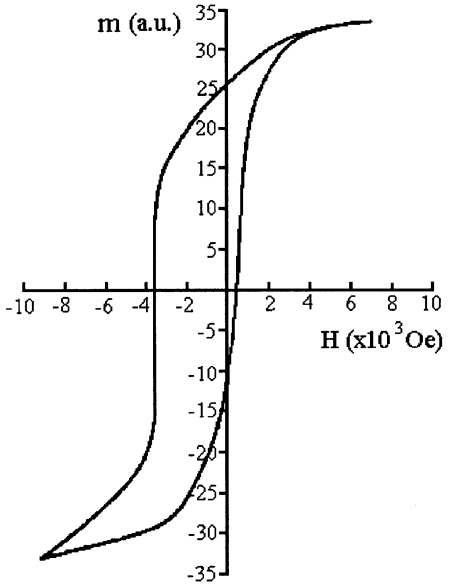

Fig. 5. Hysteresis loop, $m(H)$, of Co/CoO particles at $T = 77$ K after field cooling [11].

[3,11,26,61–64] and Co–CoN [61] large loop shifts have been reported. Shown in Fig. 5 is a shifted hysteresis loop for Co–CoO particles, with a loop shift of 1600 Oe [11].

It is noteworthy that loop shifts and increase in coercivity have also been found in pure ferri or AFM nanoparticles [104,105]. These effects are probably related to the surface layer of the particles, which due to the changes in the atomic coordination form a layer of disordered spins (i.e. spin glass layer). Therefore, in practice, the particles behave as two magnetic systems [104,105].

In small particles, due to the difficulty of determining the exact FM and AFM thicknesses, it is difficult to compare quantitatively the results between different systems. Moreover, these systems are not ideal for studies of fundamental aspects of exchange bias, because: distribution of particle sizes and shapes is always present, the difficulty to identify the nature of the interface, stoichiometry, crystallinity, etc. of the AFM layers.

3.2. Inhomogeneous materials

There are many systems which exhibit exchange bias without clearly defined AFM–FM interfaces or which have multiple random AFM–FM interfaces. We denote as *materials without well defined interfaces*, materials with competing magnetic interactions, where due to the arrangement of the magnetic ions, different areas (or domains) with AFM or FM interactions are created. This category comprises spin glasses and some ferrimagnets. We have labeled these materials as 'inhomogeneous materials'. Due to the nature of these materials, it is difficult to extract much useful basic information about exchange bias. Therefore, we feel that it is beyond the scope of this review to analyze in detail this broad subject. However, a brief overview of these materials is given below.

Spin glasses have been thoroughly studied for many years [312,313], and many systems are known to exhibit exchange bias properties, such as loop shifts [8,10,312,313] (Fig. 6) or sin ϕ component in the torque [8,10]. Probably the most studied systems are alloys containing Mn, such as $Cu_{1-x}Mn_x$ [28,29], $Ag_{1-x}Mn_x$ [29] or $Ni_{1-x}Mn_x$ [30,67]. However, exchange bias effects have been observed in other spin glass systems, such as $Au_{1-x}Fe_x$ [235]. In some of the above systems exchange bias properties have been observed in polycrystalline [29,30], single crystal [28] and thin film form [67], indicating that this is an intrinsic property of the material, rather than a sample preparation artifact. The exchange bias properties of this kind of spin glass materials have been modeled rather successfully [8,314].

Another important group of spin glasses, which also exhibit exchange bias properties, are amorphous materials, especially Fe and Mn based amorphous materials, e.g. $Fe_{1-x}Zr_x$ [236] or $(Ni_{1-x}Mn_x)_{75}P_{16}B_6Al_3$ [68]. Other more common amorphous ferromagnetic materials, occasionally show loop shifts especially after annealing. However, this could be due to nano-precipitates of hard magnetic materials [31], which would cause similar shifts of the loops.

Occasionally, spin glasses are one of the components of bilayers of the type FM–spin glass or ferri–spin glass. In such systems, the AFM rich areas of the spin glass not only couple to the FM rich areas of the spin glass but also to the FM or ferri adjacent layer. Thus, the FM (ferri) layer exhibits exchange bias properties. However, due to

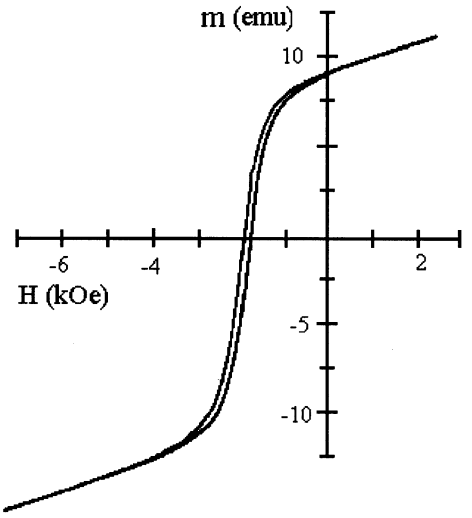

Fig. 6. Hysteresis loop, $m(H)$, of a polycrystalline $Ag_{80}Mn_{20}$ spin glass at $T = 1.8$ K after field cooling [8].

the nature of these materials the overall effects are rather small. Two of these systems have been reported in the literature, Fe/NiMn (FM–spin glass) [244] and $NiFe_2O_4$/amorphous–$NiFe_2O_4$ (ferri–spin glass) [69]. However, due to the random nature of the spin glasses and the fact that the spin glass layer can exhibit exchange bias effects by itself, it is rather difficult to extract quantitative information from such systems.

Bulk ferrimagnets with exchange bias have not been systematically studied, however, several examples have been reported in the literature. Exchange bias properties have been observed in different types of ferrimagnets such as amorphous rare-earth based alloys, like TbFe [237] or GdCo [32], oxide type ferrimagnets, like Co_2TiO_4 [33] of $CoCr_2O_4$ [70], and diluted or substituted compounds such as $Li_{0.5}Fe_{2.5-x}Ga_xO_4$ [111].

The other major group among the inhomogeneous materials, are materials with multiple random AFM–FM interfaces, which are mainly polycrystalline materials with a mixture of AFM (or ferri) and FM components. One of the most studied in this group is Co sputtered in low oxygen pressure atmosphere, where Co rich and CoO rich areas are formed [21,112]. Other examples in this group are co-sputtered CoCr [113] or NiO with $NiFe_2O_3$ precipitates [245].

3.3. Coated antiferromagnetic single crystals

In order to better understand the fundamental aspects of exchange bias, several groups have studied a more controlled type of system, namely an AFM single crystal polished along a specific crystallographic direction, coated with an FM material. This procedure allows for a more controlled AFM–FM interface than the two previous types of systems. Although these systems have the potential to clarify some of the questions surrounding exchange bias, only three different AFM materials have been studied so far, CoO [12,34,71,186], NiO [13,187,238,307] and FeF_2 [72,73].

The two main aspects of exchange bias studied in coated single crystals are the role of the spin configration at the interface (by selecting different crystallographic directions) [12,13,34,72,186,187,238] and the role of the roughness (by controllably damaging the AFM surface before depositing the FM) [12,72,73].

Contrary to expectations, some of the results obtained on coated AFM crystals are rather puzzling. First, despite the presumed controlled interface of this type of systems, the exchange bias exhibited by all three systems is substantially smaller than the one obtained in small particles or thin films [12,13,34,71–73,186,187,238]. It is possible that the AFM surface is contaminated before transferring the single crystal to the deposition chamber. However, the samples are usually annealed and sometimes ion-bombarded until well defined LEED (low energy electron diffraction) and/or RHEED (reflection high energy electron diffraction) diffraction patterns are obtained. Second, there seems to be very little dependence of the exchange bias on the spin configuration of the AFM at the interface. For example, exchange bias appears to be insensitive whether the spins at the interface are *compensated* (i.e. both AFM spin sublattices present at the interface, thus the same number of spins pointing in one direction as in the opposite, see Fig. 7a) or *uncompensated* [12,13,34,72,73,186,187,238] (i.e. only one AFM spin sublattice present at the interface, thus all spins pointing in the same direction, see Fig. 7b) (see Section 6.2.1 for more details). This could be due to the reorientations of the spins at the interface, the formation of magnetic domains in the

AFM or other factors discussed later in the paper (Section 6).

Another interesting result, hinted in CoO crystals [71] and confirmed in FeF_2 crystals [72,73], is the fact that the FM layer appears to orient itself perpendicular to the anisotropy direction of the AFM spins at the interface, for compensated and uncompensated AFM surfaces. In the case of FeF_2, the easy axis of the FM layers rotates 90° between $T > T_N$ and $T < T_N$ [72,73] in order to attain this coupling. These results will be discussed in more detail in Section 6.1.

Additionally, the magnitude of the exchange bias becomes larger as the interface roughness increases for both uncompensated CoO [12] and compensated FeF_2 [72]. These results are intuitive for compensated AFM surfaces, however they are harder to interpret for uncompensated AFM surfaces. The effect of the roughness in exchange bias will be further discussed in Section 6.3.

Finally, the loops of the compensated FeF_2 (1 1 0) surface, shift towards the same direction as the cooling field [72,73], contrary to what has been observed in all other systems [1–10]. This interesting effect will be discussed in Section 6.8.

3.4. Thin films

Exchange bias materials, in thin film form, have been the most widely studied type of system. From the basic point of view, in these systems the interface can be quite effectively controlled and characterized [15,74]. From the applied point of view, most of the device applications based on exchange bias are in thin film form [17,18]. Moreover, materials in thin film form have been the basis of many interesting phenomena related to exchange bias, such as AFM thickness [140], interface disorder [74] or orientation dependence of H_E [15], to name a few. Among the layered systems, AFM–FM interfaces are the most commonly investigated, however related systems such as ferri–FM [20], AFM–ferri [19], ferri–ferri [114] have also been studied. The AFM–FM group can be divided in three main categories depending on the type of AFM used: *oxide*, *metallic*, *others*.

To compare different systems, independent of the ferromagnetic material and its thickness, the magnitude of the exchange bias is described in terms of an interface energy per unit area

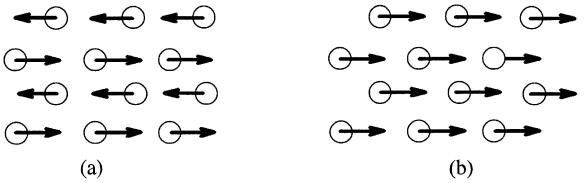

Fig. 7. Schematic spin diagram for a (a) compensated and (b) uncompensated AFM surface.

$$\Delta E = M_{FM} t_{FM} H_E, \quad (1)$$

where M_{FM} and t_{FM} are the saturation magnetization and thickness of the ferromagnet and H_E is the exchange bias magnitude. Note that following common practice we will assume that ΔE depends only on the saturation magnetization and not the type of FM material. In the tables comparing different AFM materials we will use this kind of notation. In the following tables, the temperature at which H_E becomes zero, usually called the blocking temperature, T_B, is also given. This property will be discussed in more detail later in Section 6.5.

3.4.1. Oxide AFMs

Following the work on oxidized FM particles, most of the early work on exchange bias on thin films was on oxidized transition metal films, Co–CoO [16,35,36,58,75,76,78,79,115,190,205,216–218,229–231,239,299,303,309], Ni–NiO [216,217,239,240,246], Fe–FeO [77,80,294,295] or oxidized $Fe_{20}Ni_{80}$ [37,117,188,189,227,260]. Similarly to oxidized particles, oxidized Co films exhibit rather large exchange bias [16,35,36,75,76,78,79,115,190,216–218,229–231,239] (Table 2), while oxidized Ni and Fe films usually show smaller loop shifts [77,80,216,217,239,240,246,294,295] (Table 2). However, this kind of samples are difficult to compare. Although the oxide layer can be measured quite accurately, the films may tend to oxidize through the grain boundaries, thus increasing the interface surface. Furthermore, the oxide is usually polycrystalline, and sometimes multiphase [16]. However, as can be observed in Table 2, oxidized Co films are the systems exhibiting the largest interface energy, $\Delta E = 3.5$ erg/cm^2 at 10 K [229].

Table 2
Compilation of interface energies, $\Delta E = H_E t_{FM} M_{FM}$, blocking temperatures, T_B, and bulk Néel temperatures, T_N, for oxide antiferromagnets used in exchange bias. Note that ΔE values are at room temperature unless otherwise stated. Note that whenever possible we have limited ourselves to thick enough AFM layers, where H_E and T_B are independent of t_{AFM}

Material	ΔE (erg/cm^2)	T_B (K)	T_N (K)
NiO (oxid)[a]	0.05–0.29	–	
NiO (poly)[b]	0.007–0.09	450–480	
NiO (1 1 1)[c]	0.004–0.06	450–500	520
NiO (1 1 1) (10 K)[d]	0.31	450–500	
NiO (1 0 0)[e]	0.02–0.16	480	
NiO (1 1 0)[f]	0.05	–	
CoO (oxid) (10 K)[g]	0.40–3.50	200–290	
CoO (oxid) (77 K)[h]	0.16–0.40	200–290	
CoO (poly) (10 K)[i]	0.03–0.12	290	290
CoO (poly) (150 K)[j]	0.10–0.28	290	
CoO (poly-multi) (100 K)[k]	0.84	260	
CoO (1 1 1) (77 K)[l]	0.14–0.48	290	
$Co_xNi_{1-x}O$ (poly)[m]	0.09	370	290–520
$Co_xNi_{1-x}O$ (1 1 1)[n]	0.04–0.06	390–430	
CoO/NiO (poly-multi)[o]	0.06–0.12	380–410	290–520
FeO (oxid) (10 K)[p]	0.05–0.10	100	200
Fe_2O_3 (poly)[q]	0.003–0.07	450–620	
Fe_2O_3 (0 0 0 1)[r]	0.0	–	950
Fe_2O_3 (1 1 $\bar{2}$ 0)[s]	0.0	–	
$Fe_xNi_{1-x}O$ (oxid) (77 K)[t]	0.02–0.08	40–200	200–520
Cr_2O_3 (poly)[u]	0.003	–	310

[a]AFM layer obtained from the oxidation of Ni layers [216,217].
[b]Polycrystalline AFM layers [81–83,115,116,120–123,125–128,180,182,192–195,199,215,271–275,288,290,308].
[c]AFM layers with (1 1 1) texture [122,130,131,180,192,193,195–198,271,273].
[d]AFM layers with (1 1 1) texture measured at $T = 10$ K [131].
[e]AFM layers with (1 0 0) texture [122,124,125,129,193,273,276].
[f]AFM layers with (1 1 0) texture [273].
[g]AFM layer obtained from the oxidation of Co layers, measured at $T = 10$ K [35,36,75,76,229–231].
[h]AFM layer obtained from the oxidation of Co layers, measured at $T = 77$ K [16,58,78,79,190,205,216–218].
[i]Polycrystalline AFM layers, measured at 10 K [102].
[j]Polycrystalline AFM layers, measured at 150 K [172,173].
[k]Co–CoO multilayers with polycrystalline AFM layers, measured at $T = 100$ K [38].
[l]AFM layers with (1 1 1) texture measured at $T = 77$ K [118,119,169].
[m]Polycrystalline AFM layers [115].
[n]AFM layers with (1 1 1) texture [220,221].
[o]AFM layer comprised of CoO/NiO multilayers [41,134–136].
[p]AFM layer obtained from the oxidation of Fe layers, measured at $T = 10$ K [77,80].
[q]Polycrystalline AFM layers [39,132,133,195,219,247,293].
[r]AFM layers with (0 0 0 1) texture [293].
[s]AFM layers with (1 1 $\bar{2}$ 0) texture [293].
[t]AFM layer obtained from the oxidation of $Fe_{20}Ni_{80}$ layers [37,117,188,189,227].
[u]Polycrystalline AFM layers [190,218].

To avoid some of these problems, antiferromagnetic oxides have been sputtered directly from the oxide or in a reactive oxygen atmosphere. Besides the work on CoO [38,102,118,119,169,172,173] and Cr_2O_3 [190,218] AFMs (Table 2), the recent interest in NiO [81–83,106,115,116,120–131,136,180, 185,192–199,215,271–276,288,290,305,306,308], α-Fe_2O_3 [39,132,133,195,219,247,293], $Co_xNi_{1-x}O$ [40,115,220,221,261,311] and CoO/NiO multilayers [41,134–136], with T_N well above room temperature, has been steadily increasing (Table 2), mainly due to their increased corrosion resistance [215,274].

Surprisingly, well oriented AFM oxides can exhibit smaller exchange bias than oxidized metallic layers or polycrystalline AFM layers (Table 2), probably due to oxidation through grain boundaries, increasing the effective interface area or other magnetic or microstructural factors.

3.4.2. Metallic AFMs

In 1964, the first fully metallic thin film system was reported [200]. $Fe_{20}Ni_{80}$/Mn bilayers were annealed to enhance diffusion, thus creating antiferromagnetic $Fe_xNi_yMn_{1-x-y}$ compounds at the interface, with $T_B > 300$ K [39,58,137,190,191, 200–204,206,207,218,248–254,296–300,303,304]. This evolved into one of the most studied AFM systems in exchange bias films, $Fe_{50}Mn_{50}$ [15,39, 42–47,59,60,84–87,127,138–144,146–153,155,175, 176,181,182,208,209,219,222–225,241,242,247,255–259,262–264,270,274,277–282,289,291,292,301]. The latter was the basis for most exchange biased GMR spin valves until recently [47,149–153,225, 274,277–282,289,291,292]. Another compound derived from the original metallic system, Ni_xMn_x [48–51,88–90,127,156,158–161,163,168,171,178], has started to gain interest, again for its T_N above room temperature and its superior corrosion resistance as compared to $Fe_{50}Mn_{50}$ [163].

The prospective applications of spin valves has motivated research on new metallic AFM, with high T_N and good corrosion properties, such as $Cr_xMn_yM_{1-x-y}$, where M = Pt, Rh, Cu, Pd, Ir, Ni, Co, Ti [39,144–146,154,164,174,183,210–212,283], $Pd_xPt_yMn_{1-x-y}$ [106,156,157,165,177,284], Co_xMn_x [170], $Fe_xMn_yRh_{1-x-y}$ [57,179] or Cr_xAl_{1-x} [56,162,184]. Moreover, other AFM systems such as pure Cr [213,226] or Mn [88,89,109] have also been studied.

The systems based on metallic AFMs studied to date are summarized in Table 3.

3.4.3. Other AFMs

Other, non-metallic or non-oxide systems exhibiting exchange bias include sulfides, fluorides and nitrides. The first of such systems was FeS [52,58,299]. The studies on this system were carried out by sulfading the surface of an Fe film. Like in oxidized films, it is difficult to compare with other systems since the details of the structure are not clear. Recently, FeF_2 [25,72,74,91,92,232,310] and MnF_2 [93] have been studied in detail (Table 4). Due to their simple spin structure these systems are certainly suitable to study basic properties of exchange bias. Another system studied due to its high T_B and corrosion resistance is CrN [103].

3.4.4. Ferrimagnets

Several systems which have a ferrimagnet as part of the exchange bias couple have been reported in the literature. Due to their magnetic structure, ferrimagnets can play either the role of the AFM or FM in bilayer systems. FM–ferri ($Fe_{20}Ni_{80}$–TbCo [20,53,285–287,302], $Fe_{20}Ni_{80}$–DyCo [54], $Fe_{20}Ni_{80}$–TbFe [55,166] and Fe–Fe_3O_4 [94]) or ferri–AFM (Fe_3O_4–CoO [19,95,101,167,265] and Fe_3O_4–NiO [96–98,265–269]) and even ferri–ferri (TbFeCo–TbFeCo [114,214] and $CoFe_2O_4$–$(Mn,Zn)Fe_2O_4$ [99,100]) systems may exhibit large exchange bias (Table 5). To the best of our knowledge, Fe_3O_4/CoO (ferri–AFM) has the largest exchange bias reported to date for any *bilayer* system (excluding oxidized Co films), with $\Delta E = 2.2$ erg/cm^2 at 10 K [19]. Systems containing ferrimagnets, in at least one of their components, are difficult to analyze theoretically, mainly due to the added complexity of the two different magnetic sublattices in the ferrimagnet [20,54,315].

4. Applications

Materials exhibiting exchange bias and related effects have been proposed and utilized in several

Table 3
Compilation of interface energies $\Delta E = H_E t_{FM} M_{FM}$, blocking temperatures, T_B, and bulk Néel temperatures, T_N, for metallic antiferromagnets used in exchange bias. Note that ΔE values are at room temperature unless otherwise stated. Note that whenever possible we have limited ourselves to thick enough AFM layers, where H_E and T_B are independent of t_{AFM}

Material	ΔE (erg/cm^2)	T_B (K)	T_N (K)
$Fe_{50}Mn_{50}$ (poly)[a]	0.02–0.20	390–470	
$Fe_{50}Mn_{50}$ (poly-ann)[b]	0.05–0.47	420–570	
$Fe_{50}Mn_{50}$ (1 1 1)[c]	0.01–0.19	380–480	490
$Fe_{50}Mn_{50}$ (1 1 1-ann)[d]	0.05–0.16	–	
$Fe_{50}Mn_{50}$ (1 0 0)[e]	0.04–0.07	–	
$Fe_{50}Mn_{50}$ (1 1 0)[f]	0.04–0.06	–	
$Ni_{50}Mn_{50}$ (poly)[g]	0.002	770	
$Ni_{50}Mn_{50}$ (poly-ann)[h]	0.16–0.46	770	1070
$Ni_{50}Mn_{50}$ (1 1 1-ann)[i]	0.10–0.36	520–650	
$Ni_{25}Mn_{75}$ (1 1 1-ann)[j]	0.07	420	–
$Fe_xNi_yMn_{1-x-y}$ (poly)[k]	0.03–0.16	470–620	–
FeMnRh (poly)[l]	0.05	420	–
FeMnRh (poly-ann)[m]	0.06	420	
Rh_xMn_{1-x} (poly)[n]	0–0.13	–	–
Co_xMn_{1-x} (poly)[o]	0.14	–	–
α-Mn (poly) (5 K)[p]	0.08–0.2	50	95
Cr (poly) (4 K)[q]	0.002	–	310
Cr (1 0 0) (4 K)[r]	0	130	
$Cr_{1-x}Mn_x$ (poly)[s]	0.02	450	–
$Cr_xMn_yPt_{1-x-y}$ (poly)[t]	0.08	600	–
$Cr_xMn_yPt_{1-x-y}$ (poly-ann)[u]	0.16–0.35	600	
$Cr_xMn_yRh_{1-x-y}$ (poly)[v]	0.05–0.08	620	–
$Cr_xMn_yCu_{1-x-y}$ (poly)[w]	0.04–0.05	570	–
$Cr_xMn_yPd_{1-x-y}$ (poly)[x]	0.06–0.08	650	–
$Cr_xMn_yIr_{1-x-y}$ (poly)[y]	0.04	550	–
$Cr_xMn_yNi_{1-x-y}$ (poly)[z]	0.03	–	–
$Cr_xMn_yCo_{1-x-y}$ (poly)[a1]	0.03	–	–
$Cr_xMn_yTi_{1-x-y}$ (poly)[b1]	0.003	–	–
Pt_xMn_{1-x} (poly-ann)[c1]	0.02–0.32	400–650	480–980
Pd_xMn_{1-x} (poly)[d1]	0.06	–	–
$Pd_xPt_yMn_{1-x-y}$ (poly)[e1]	0.08–0.11	570	–
Ir_xMn_{1-x} (1 1 1)[f1]	0.01–0.19	400–520	690
Cr_xAl_{1-x} (1 1 0)[g1]	0.01–0.04	550	900

[a]Polycrystalline AFM layers [39,84,86,127,138,142,148,152,208,219,222,224,247,255–257,259,292].
[b]Polycrystalline AFM layers after annealing [43,45,46,87,139,222,274].
[c]AFM layers with (1 1 1) texture [15,42,44,47,59,60,85,128,138,141,143,144,146,147,149–152,155,175,176,181,182,209,223,225,277–279, 282,289,291].
[d]AFM layers with (1 1 1) texture after annealing [140,279].

different applications since their discovery [6,17,18, 22,316–319].

The enhanced coercivity of small oxidized particles provides the first potential technological application of exchange bias, as permanent magnet materials [6] and high density recording media [64,66]. Some inhomogeneous materials (e.g. Co–CoO) were also suggested as candidates for perpendicular magnetic recording media [21,32, 112,113].

However, most industrial applications based on exchange bias are in thin film form [17,18,22, 316–319]. The first proposed application of exchange bias in bilayers was as magnetic recording media. Small areas of an FM–AFM bilayer were heated up to $T_N < T < T_C$ in the presence of a field opposite to the exchange bias field, thus, forming areas with reversed magnetization to the overall magnetization of the film [22,320]. Another proposed application is as domain stabilizer in recording heads based on anisotropic magnetoresistance. An AFM layer is deposited on the edges of the FM layer, to avoid closure domains, and thus reduce the Barkhausen noise of the devices [18,39,48,160, 215,241,321–325]. Recently, exchange bias became part of a new class of 'spin-valve' devices, based on giant magnetoresistance (GMR) [17,23,316–319, 326]. This type of device consists typically of two FM layers separated by a non-magnetic layer. One of the FM layers is grown on, or covered by, an AFM layer (Fig. 4a) [23,326]. The FM ('pinned' layer) in contact with the AFM layer has a shifted loop, however, the other FM ('free' layer) has a conventional hysteresis loop (Fig. 4b) [23,326]. Thus there is a field range where the FM layers have antiparallel magnetizations (Fig. 4b) [23]. Due to the spin dependent scattering, when the magnetizations in the layers are parallel the resistance is low, but when they are antiparallel the resistance is high (Fig. 4c) [23,326]. What makes these devices

Table 3 footnotes (*Continued*):
[e]AFM layers with (1 0 0) texture [15,138,209].
[f]AFM layers with (1 1 0) texture [15,138,209].
[g]Polycrystalline AFM layers [127].
[h]Polycrystalline AFM layers after annealing [48,127,156,160,161,163].
[i]AFM layers with (1 1 1) texture after annealing [49,50,161,168,178].
[j]AFM layers with (1 1 1) texture after annealing [51,88–90,158,159,171].
[k]AFM layer obtained by diffusion of Mn in $Fe_{20}Ni_{80}$ due to high temperature annealing [39,137,190,191,200–203,206,207,218, 248–250,252].
[l]Polycrystalline AFM layers [179].
[m]Polycrystalline AFM layers after annealing [179].
[n]Polycrystalline AFM layers (a range of compositions has been studied) [57].
[o]Polycrystalline AFM layers [170].
[p]Polycrystalline AFM layers, measured at $T = 5$ K [88,89,109].
[q]Polycrystalline AFM layers, measured at $T = 4$ K [226].
[r]AFM layers with (1 0 0) texture, measured at $T = 4$ K [213].
[s]Polycrystalline AFM layers (a range of compositions has been studied) [210,211].
[t]Polycrystalline AFM layers (a range of compositions has been studied) [164,210–212].
[u]Polycrystalline AFM layers after annealing (a range of compositions has been studied) [131,164].
[v]Polycrystalline AFM layers (a range of compositions has been studied) [210,211].
[w]Polycrystalline AFM layers (a range of compositions has been studied) [210,211].
[x]Polycrystalline AFM layers (a range of compositions has been studied) [210,211].
[y]Polycrystalline AFM layers (a range of compositions has been studied) [211].
[z]Polycrystalline AFM layers (a range of compositions has been studied) [210].
[a1]Polycrystalline AFM layers (a range of compositions has been studied) [210].
[b1]Polycrystalline AFM layers (a range of compositions has been studied) [210].
[c1]Polycrystalline AFM layers (a range of compositions has been studied) [106,165,284].
[d1]Polycrystalline AFM layers (a range of compositions has been studied) [156].
[e1]Polycrystalline AFM layers (a range of compositions has been studied) [156,157,177].
[f1]AFM layer with (1 1 1) texture (a range of compositions have been studied) [144–146,154,174,183,283].
[g1]AFM layer with (1 1 0) texture [56,162,184].

Table 4
Compilation of interface energies, $\Delta E = H_E t_{FM} M_{FM}$, blocking temperatures, T_B, and bulk Néel temperatures, T_N, for non-metallic, non-oxide antiferromagnets used in exchange bias. Note that ΔE values are at $T = 10$ K. Note that whenever possible we have limited ourselves to thick enough AFM layers, where H_E and T_B are independent of t_{AFM}

Material	ΔE (erg/cm^2)	T_B (K)	T_N (K)
FeS (poly)[a]	0.11	540	610
FeF_2 (1 1 0)[b]	0.5–1.3	79	
FeF_2 (1 0 1)[c]	0.2–0.4	79	79
FeF_2 (0 0 1)[d]	0.002	79	
MnF_2 (1 1 0)[e]	0.05–0.10	67	67
CrN (poly)[f]	0.3–0.4	200	260

[a]AFM layer obtained from sulfading a Fe layer [52].
[b]AFM layer with (1 1 0) texture [72,74,91,92].
[c]AFM layer with (1 0 1) texture [72].
[d]AFM layer with (0 0 1) texture [72].
[e]AFM layer with (1 1 0) texture [93].
[f]Polycrystalline AFM layer [103].

Table 5
Summary of interface energies $\Delta E = H_E t_{FM} M_{FM}$, blocking temperatures, T_B, for bilayers having a ferrimagnet as part of the exchange bias couple

Material	ΔE (erg/cm^2)	T_B (K)
FM–ferri		
TbCo (amorph)[a]	0.08–0.70	420–450
TbFe (amorph)[b]	0.08	420
DyCo (amorph)[c]	0.08–0.70	–
Fe_3O_4 (poly)[d]	0.35	–
ferri–AFM		
Fe_3O_4/CoO (1 1 1) (10 K)[e]	2.20	290
Fe_3O_4/CoO (1 0 0) (10 K)[f]	1.43	290
Fe_3O_4/CoO (1 0 0-multy) (77 K)[g]	0.7–1.27	320–450
Fe_3O_4/NiO (1 0 0-multy)[h]	0.05	–
Fe_3O_4/NiO (1 0 0-multy) (30 K)[i]	0.35	–

[a]Amorphous ferri layer [20,53,219,285–287].
[b]Amorphous ferri layer [55,166].
[c]Amorphous ferri layer [54].
[d]Polycrystalline ferri layer [94].
[e]AFM layer with (1 1 1) texture, measured at $T = 10$ K [95]
[f]AFM layer with (1 0 0) texture, measured at $T = 10$ K [19,95].
[g]Fe_3O_4/CoO multilayers with the AFM layer with (1 0 0) texture, measured at $T = 77$ K [101,167].
[h]Fe_3O_4/NiO multilayers with the AFM layer with (1 0 0) texture [266,267].
[i]Fe_3O_4/NiO multilayers with the AFM layer with (1 0 0) texture, measured at $T = 30$ K [98].

attractive for applications is that the low to high resistance changes occur at rather low fields [17,316–319]. Since the discovery of GMR in exchange bias spin valves, a variety of devices have been built and proposed [17,316–319], such as read-heads [135,272,278,283,284,287,288], magnetic sensors [127,278,282,285,286,327,328] or magnetoresistive memories [329–331].

Most applications are not limited to AFM–FM type interfaces. FM–ferri systems have also been utilized in similar applications, especially in GMR type devices [285–287,329], domain stabilizers [332], and as recording media [32,214]. It is beyond our scope to review GMR devices which use exchange bias. However, whenever articles concerning GMR [41,47,53,75,81,121,128,132,133,136,149,151,152,164,168,177,178,183,199,271,273–275,279–281,289–293] and GMR devices [127,135,179,272,278,283–288] include some information related to exchange bias itself, they have been included in this review.

5. Theoretical models

In the introduction, we have presented an intuitive model to explain the origin of the exchange bias. In this model, the energy per unit area of an exchange bias system, assuming coherent rotation of the magnetization, can be written [1] as

$$E = -HM_{FM}t_{FM}\cos(\theta-\beta) + K_{FM}t_{FM}\sin^2(\beta) + K_{AFM}t_{AFM}\sin^2(\alpha) - J_{INT}\cos(\beta-\alpha), \quad (2)$$

where H is the applied field, M_{FM} the saturation magnetization, t_{FM} the thickness of the FM layer, t_{AFM} the thickness of the AFM layer, K_{FM} the anisotropy of the FM layer, K_{AFM} the anisotropy of the AFM layer and J_{INT} the interface coupling constant. β, α and θ are the angles between the magnetization and the FM anisotropy axis, the AFM sublattice magnetization (M_{AFM}) and the AFM anisotropy axis, and the applied field and the FM anisotropy axis (see Fig. 8) [1]. Note that the AFM and FM anisotropy axes are usually assumed to be in the same direction (i.e. collinear). The first term in the energy equation accounts for the effect of the applied field on the FM layer, the second

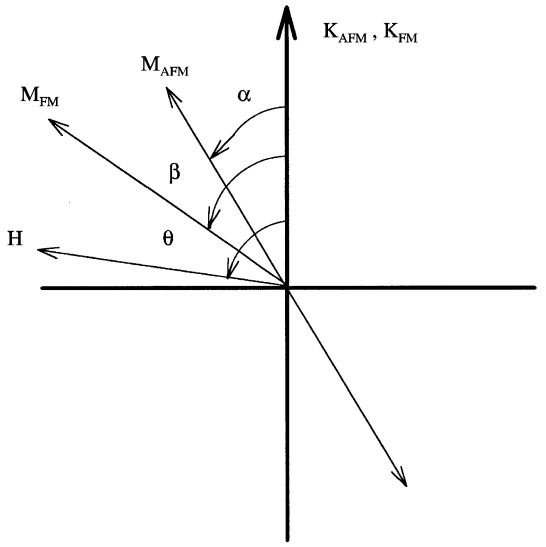

Fig. 8. Schematic diagram of angles involved in an exchange bias system. Note that the AFM and FM anisotropy axes are assumed collinear and that the AFM sublattice magnetization M_{AFM} has two opposite directions.

term is the effect of the FM anisotropy, the third term takes into account the AFM anisotropy and the last term takes into consideration the interface coupling. Although this energy function takes into account the main parameters involved in exchange bias, it assumes: the absence of AFM and/or FM domains, that the AFM and FM anisotropy axes are parallel and ferromagnetic coupling at the interface.

In the simplest case the FM anisotropy is assumed to be negligible [1] (the condition $K_{FM}t_{FM} \ll K_{AFM}t_{AFM}$ is often fulfilled experimentally), thus the energy becomes

$$E = -HM_{FM}t_{FM}\cos(\theta - \beta) + K_{AFM}t_{AFM}\sin^2(\alpha) - J_{INT}\cos(\beta - \alpha). \quad (3)$$

Minimizing the energy with respect to α and β, the loop shift is found to be [1]

$$H_E = \frac{J_{INT}}{M_{FM}t_{FM}}. \quad (4)$$

Another important result from this minimization is that the condition

$$K_{AFM}t_{AFM} \geqslant J_{INT} \quad (5)$$

is required for the observation of exchange anisotropy [1]. If $K_{AFM}t_{AFM} \gg J_{INT}$ then the system is minimized by keeping α small independently of β. However, if $J_{INT} \gg K_{AFM}t_{AFM}$ it is energetically more favorable to keep $(\beta - \alpha)$ small, i.e. AFM and FM spins rotate together. In other words, if the above condition is not satisfied, the AFM spins follow the motion of the FM layer, thus no loop shift should be observed, only an increase in coercivity.

The exchange bias magnitude predicted by these calculations depends on the assumed value for J_{INT}. If J_{INT} is taken to be similar to the ferromagnetic exchange, H_E is predicted to be several orders of magnitude larger than the experimental result [15]. To account for these discrepancies, different approximations of the energy equation have been used to model the hysteresis loops [102,203,207, 301,333–350], and torque magnetization (rotational hysteresis) [13,345–347], of exchange bias systems. These studies attempt to account for different important parameters in exchange bias systems which are not considered in the basic formula. These include the formation of domains in the AFM [333,345–347,351], or FM layer [206,337–339,345–347,351], field effect on the AFM layer [13,341–343], grain size distribution [60,344], induced thermoremanent magnetization in the AFM layer [345–347], non-collinearity of AFM–FM spins [348,349], random anisotropy in the AFM layer [350] or uncompensated surface spins [102]. Introducing time dependent terms in the magnetization allows modeling some aspects of ferromagnetic resonance through similar equations [251,338,339,352–354].

These models have attained different degrees of agreement with existing experimental results. Often the individual approximations apply for a specific system and are not valid for other systems. Furthermore, most of the models assume: the interface plane to be homogeneous (i.e. they are unidimensional), the AFM and FM anisotropy axes to be collinear and/or that the AFM moments at the interface are uncompensated. Moreover, band structure calculations of AFM–FM interfaces have been used to predict the exchange interactions at the interface, and thus the existence of exchange bias [356–358].

Finally, in a recent model in which the quantum mechanical hamiltonian is solved for spin compensated AFM surfaces, H_E arises from spin waves transmitted across the interface [355]. However, this model is unidimensional and assumes collinear spins.

5.1. AFM domains

Some models stress the importance of AFM domains on exchange bias [333,345–347,359–362]. One of the models assumes the formation of AFM domains *perpendicular* to the interface plane due to the random field created by roughness (or other defects), and that it is the contribution of energy difference between the different random domains which produces exchange bias [359–361]. This model takes into account the two-dimensionality of the interface, and is, to some extent, independent of the collinearity of the spins and the uncompensated–compensated AFM spins [359–361]. Two other models claim that the formation of AFM domains *parallel* to the interface when the FM layer rotates can also cause exchange bias [333,362]. Both of these models suffer from the drawback, that they assume uniform properties for the interfacial plane [333,362]. One of these models assumes uncompensated AFM surfaces and collinear AFM–FM spins at the interface [333], while the other is independent of the spin configuration (compensated–uncompensated) and allows for the possibility of non-collinearity [362].

5.2. Perpendicular coupling

In a recent micromagnetic calculation [362] for a compensated surface, the interfacial energy is minimized for perpendicular coupling between the FM and AFM layers. The interfacial coupling occurs between the FM and a small canting of the compensated AFM surface. This model has claimed to explain a large H_E in fully compensated FeF_2 surfaces and the existence of a positive H_E as will be discussed in the next section [362].

6. Unsolved issues

There are many experimental aspects of exchange bias which have not been studied in detail, are still controversial or unresolved. In this section we discuss some of these issues.

6.1. Thickness dependence

The role of the thickness of the AFM and FM layers in exchange bias bilayers has been studied in detail. Here we discuss the main results concerning the effects of the FM and AFM thickness on exchange bias.

6.1.1. FM thickness

For all the systems studied, it has been observed that exchange bias is roughly inversely proportional to the thickness of the FM layers (see for instance Fig. 9)

$$H_E \propto \frac{1}{t_{FM}} \tag{6}$$

indicating that exchange bias is an interface effect [15,16,35,37,51,54,59,74,76,80,82–84,88,103,123–125,127,140,143,148,155,156,159,160,162,171,174,176,183,208,209,216,224,246,255,257,272,279,288,289]. This relation holds for rather thick FM layers (several hundred nm [37,51,54,74,84,88,127,140,159,171,216,224,255,257]), as long as the thickness is smaller than the FM domain wall size. However, if the FM layer is too thin, the relation is no longer valid [148], probably because the FM layer becomes discontinuous. The thickness at which this occurs (usually a few nm) varies from system to system and depends on the microstructure and growth of the FM layer [15,59,80,124,127,143,148,160,209,255,279,289].

6.1.2. AFM thickness

The dependence of H_E on the AFM thickness is more complicated. The general trend is that for thick AFM layers, e.g. over 20 nm, H_E is independent of the thickness of the AFM layer. As the AFM thickness is reduced, H_E decreases abruptly and finally, for thin enough AFM layers (usually a few nm) H_E becomes zero, as shown in Fig. 10.

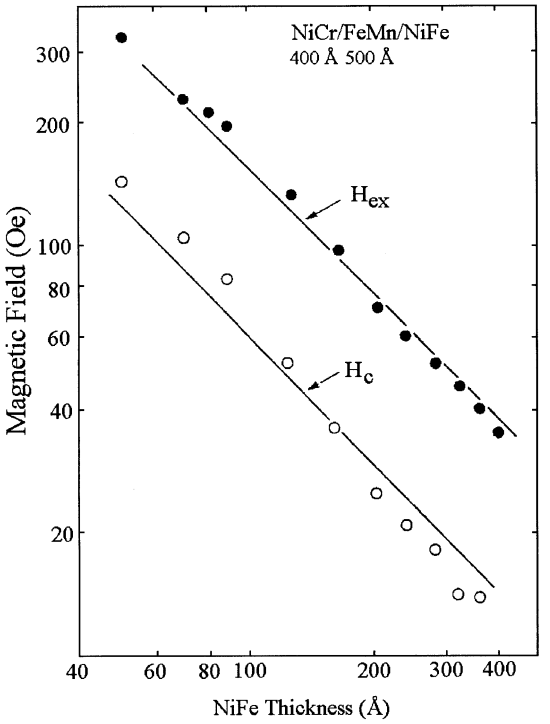

Fig. 9. Dependence of exchange bias H_E (filled symbols) and coercivity H_C (open symbols) with the FM layer thickness for $Fe_{80}Ni_{20}$/FeMn at a fixed $t_{AFM} = 50$ nm [208].

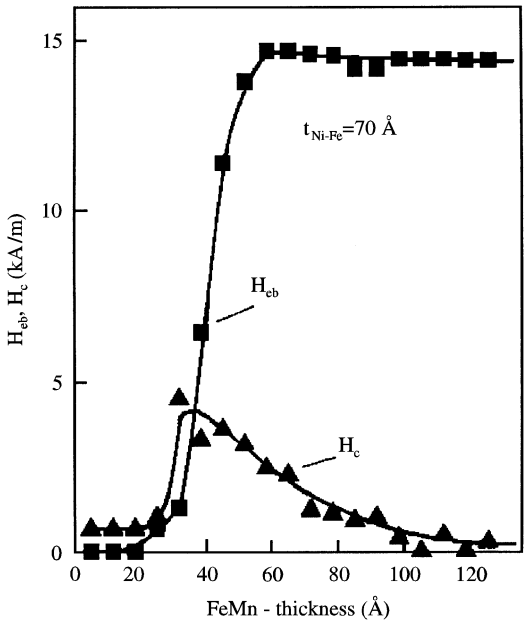

Fig. 10. Dependence of exchange bias H_E (square symbols) and coercivity H_C (triangular symbols) with the AFM layer thickness for $Fe_{80}Ni_{20}$/FeMn at a fixed $t_{FM} = 7$ nm [15]. Note that 80 A/m = 1 Oe.

The exact thickness at which the different stages in this process take place depends on the specific system, its microstructure and the measurement temperature [15,19,42,56,57,59,82,83,88,95,102,103, 120,123,127,131,136,138,140,143,144,148,149,159, 162,164,165,174,180,183–185,195,196,208–210,212, 223,255,285,286]. The decrease of H_E for thin enough AFM layers is due to several connected factors. As discussed in the theoretical part (Section 5), exchange bias requires the condition $K_{AFM}t_{AFM} \geqslant J_{INT}$ to be fulfilled. Thus as t_{AFM} is reduced this condition is violated, moreover the dependence of K_{AFM} with AFM thickness, which has not been studied in detail, may also influence H_E. Another important factor is thickness dependence of T_N, and thus the blocking temperature, T_B, of the AFM layer (discussed in Section 6.5). Therefore, for thin enough AFM layers the reduced temperature, T/T_B varies with thickness. Additionally, the AFM domain structure may also affect H_E if the thickness becomes comparable to the AFM domain wall size. Finally, decreasing the thickness of the AFM layer may change the AFM grain size which in turn influences the critical thickness at which $H_E = 0$.

There are two main discrepancies to the general behavior described above. First, in some cases there seems to be a decrease in H_E for large thicknesses, after H_E has levelled off [15,42,56,59,88,140,144, 159,184,195,209,223]. This effect is probably due to microstructural changes in the AFM layer with thickness, e.g. one type of phase or orientation is no longer stable above certain thicknesses. Second, in some systems as the thickness of the AFM layer is reduced there is a peak in H_E before the main decrease [15,19,88,95,103,120,123,127,144,149,156, 159,185,196]. This behavior has been predicted theoretically if there is a change in AFM domain structure with decreasing thickness [360]. However, some authors claim this effect to be purely structural [19].

6.2. AFM orientation

Due to the interfacial nature of exchange bias, H_E may be expected to depend strongly on spin

configuration at the AFM–FM interface. To study this effect some AFM–FM systems have been investigated using different AFM orientations [15,72,95,122,138,209,273]. Two main issues concerning the orientation have been addressed: *compensated* versus *uncompensated* [15,72,95,122,138, 209,273] AFM surfaces and *in-plane* versus *out-of-plane* [15,72,138,209] AFM spins. The main problem in this kind of studies is the difficulty to determine the exact spin configuration at the interface and therefore it is customary to assume that the bulk spin configuration is preserved. However, at the interface the AFM atoms can relax or reconstruct and AFM domains may be formed or the spins can reorient to compensate for the local structural changes. An important factor for some of these considerations is the AFM layer anisotropy, because for large anisotropy, the interfacial spins will tend to remain in their bulk configuration. Moreover, the microstructure (grain size, roughness, etc.) in the different crystalline orientations may change due to varied growth conditions and thus affect the exchange bias. Following the common practice, for the following discussion we will assume that the bulk spin structure is preserved throughout the antiferromagnet.

6.2.1. Compensated–uncompensated

In a *compensated* AFM interface the net spin averaged over a microscopic length scale is zero. Therefore, this kind of surface will have zero net magnetization (Fig. 7a). In contrast, if the spin arrangement is such that the surface magnetization is non-zero, the surface is *uncompensated* (Fig. 7b).

Intuitively, one may expect that for compensated surfaces, the spins pinning the FM layer cancel giving rise to a net zero H_E. Note, also that a compensated surface remains compensated in the presence of unit cell random roughness, however, more complicated roughness could result in uncompensated surfaces. However, it was found that all compensated surfaces investigated experimentally, exhibit exchange bias: CoO (1 0 0) [19,95,101], NiO (1 0 0) [122,124,125,129,193,273,276], NiO (1 1 0) [273], FeF_2 (1 1 0) [72,74,91,92], FeF_2 (1 0 1) [72], MnF_2 (1 1 0) [93], FeMn (1 1 1) [15,138,209], FeMn (0 0 1) [15,138,209], even in AFM single crystals covered by FM films [12,72]. Some of these orientations exhibit very large loop shifts, often larger than uncompensated orientations of the same AFM materials (see Tables 2–5).

This effect could be due to some kind of spin re-arrangement at the interface which is usually neglected. In some cases, structural matching between the FM (or ferri) layer and the AFM layer has been claimed to be the origin of finite H_E [19,95]. Although this experimental fact appears counterintuitive, some models assign it directly or indirectly to the formation of domains in the AFM layer [359–361], non-collinear coupling at the interface [362], spin wave transfer between the FM and the AFM layer [355] or residual uncompensated spins at the interface [102].

6.2.2. Out-of-the-plane spins

Usually, the theories assume that the AFM spins at the interface lay on the interface plane. However, certain orientations of some AFM materials have spins pointing out of the interface plane if the bulk spin structure is preserved: FeF_2 (1 0 1) [72], FeF_2 (0 0 1) [72], FeMn (1 1 1) [15,138,209], FeMn (0 0 1) [15,138,209] or FeMn (1 1 0) [15, 138,209].

The H_E for different FeF_2 orientations exhibit a clear trend: when the AFM spins are in the plane (FeF_2 (1 1 0)), H_E is maximum, but when the spins are completely (90°) out of the interface plane (FeF_2 (0 0 1)), $H_E = 0$. For FeF_2 (1 0 1), with an intermediate angle, H_E is about half of the one obtained for the FeF_2 (1 1 0) case [72]. The same trend is followed by the different FeMn orientations [15,138,209], although the spin structure of FeMn is more complicated than that of FeF_2, which makes the analysis more difficult.

An intuitive explanation for this effect comes from the FM–AFM spin–spin interaction strength, given as

$$\bar{S}_{AFM} \cdot \bar{S}_{FM} = S_{AFM} S_{FM} \cos \alpha \tag{7}$$

with α the angle between both spins. If the FM spins lay in the interface plane due to shape anisotropy, α is the angle between the AFM spins and the interface plane. Therefore, for in-plane AFM spins

$$\alpha = 0^\circ \Rightarrow \cos \alpha = 1 \Rightarrow H_E \text{ maximum} \tag{8}$$

and for out-of-the-plane spins

$$\alpha = 90^\circ \Rightarrow \cos\alpha = 0 \Rightarrow H_E = 0 \quad (9)$$

as observed experimentally in the FeF_2 system.

Another possible explanation assumes that the dominant factor in H_E is AFM domain formation. Therefore, following some of the exchange bias models [333,359–361]

$$H_E \propto \sqrt{K_{AFM} A_{AFM}}. \quad (10)$$

Thus, in the case of out-of-plane AFM spins, the effective AFM in-plane anisotropy, K_{Eff}, and stiffness, A_{Eff}, would play a major role. Due to the angle of the AFM spins, the effective anisotropy and stiffness at the interface plane should scale with $\cos\alpha$, thus

$$H_E \propto \sqrt{K_{Eff} A_{Eff}} = \sqrt{K_{AFM} A_{AFM}} \cos\alpha, \quad (11)$$

leading to the same conclusions as above.

6.3. Interface disorder

In the previous section, we showed that the spin structure at the interface strongly influences exchange bias. In this section, we will discuss how different structural factors which disorder the interface (such as roughness or crystallinity) affect H_E. To investigate this, ideally it is desirable to study structural effects on H_E by varying one parameter (e.g. roughness) at a time while keeping all others constant. Unfortunately, this is very difficult for most exchange bias systems. If the roughness is changed, by controlling e.g. substrate temperature, sputtering power, sputtering rate, sputtering pressure or substrate bias, usually either the grain size or the crystallinity (or both) will change. Therefore, it is often difficult to separate the different contributions. However, in some cases one parameter changes significantly more than the others, which are then assumed to be constant. This problem is greatly reduced in AFM single crystals, where different degrees of roughness can be introduced without affecting much the grain size or crystallinity.

6.3.1. Roughness

Most investigations of the roughness role on exchange bias in textured thin films seem to agree

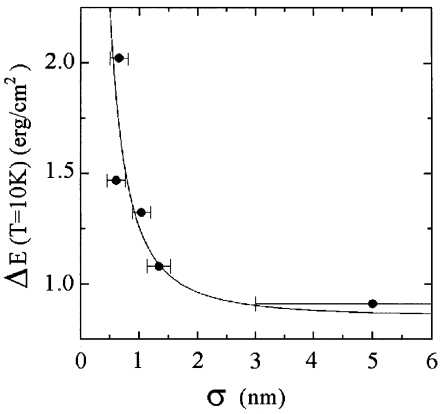

Fig. 11. Dependence of the interface energy, ΔE, at 10 K, on the interface roughness, σ, for FeF_2 (1 1 0)–Fe bilayers [92].

that the magnitude of H_E decreases with increasing roughness [72,74,92,122,138,175,197,277] (see Fig. 11), although some systems appear to be less sensitive to roughness [124,125] or behave in the opposite way [184]. This behavior appears to be independent of the interface spin structure, i.e. compensated [72,74,92,122,138,175,277], uncompensated [197] or out-of-the-plane [72,138,277]. However, the opposite effect, i.e. the magnitude of H_E increasing with increasing roughness, has been bserved for FM coated AFM single crystals (with both compensated and uncompensated surfaces [12,72]), indicating that the microstructure may play an important role. It is worth mentioning that H_E for samples with polycrystalline AFM layers appear to be less sensitive to roughness [121, 144,192].

These results can be understood, for uncompensated AFM surfaces, with the intuitive model presented in the introduction. The roughness creates areas of different spin orientation, thus the total number of spins pinning the FM in one direction is reduced, concomitantly reducing the magnitude of H_E. However, this simple reasoning is not valid for compensated surfaces, because the surface remains compensated independently of the roughness. Thus, the above conjectures imply that the magnitude of H_E should remain unchanged or even increase for compensated surfaces.

More sophisticated models assume that roughness affects the interface coupling, J_{INT}, and

consequently the magnitude of H_E [1,333,345–347, 362]. Finally, roughness may affect the formation of domains (e.g. by pinning) in the AFM layer or the amount of uncompensated surface spins and thus influence H_E [102,359–361].

6.3.2. Crystallinity

Often in thin film bilayers, the AFM layers are textured and the degree of texture ('crystallinity') may affect H_E. The crystallinity can be determined using X-ray diffraction from the full width at half maximum (FWHM) of the rocking curve, however, some information can be obtained from θ–2θ scans and transmission electron microscopy. Unfortunately, the FWHM of rocking curves for the AFM layers is rarely reported [141].

If the AFM is textured in a single orientation, generally H_E increases with increasing texture [47,50,85,141,144,145,151,153,155,174,176,177,220, 221,225,278,280], although, there are some exceptions to this trend [128,161,178]. On the other hand, as new orientations appear with changing growth conditions, H_E may change drastically without following any specific trend [126,138].

These results are related, at least in part, to the angle between the FM and AFM spins at the interface, discussed in Section 6.2. If the sample has a wider rocking curve, the different grains will have a wider range of coupling FM–AFM angles, thus reducing H_E. Another effect is that for less crystalline samples, the long range AFM properties such as the formation of domains or the anisotropy may change, thus influencing H_E.

6.3.3. Grain size

The role of the grain size (or AFM coherence length) in exchange bias remains unclear. Some of the effects of the AFM grain size are expected to be similar to the thickness effects discussed in Section 6.1.2, and will be discussed in Section 6.5, i.e. H_E and T_B should decrease with reduced AFM grain size.

The results from different studies seem to depend on the specific system and conditions, probably because as the grain size changes other parameters are also affected substantially [51,56,81,88,90,102, 145,154,171,184,192,193,199,215,291]. While H_E is reported to increase with increasing grain size for some systems [51,88,90,145,171,199,215,291], for other (or the same systems) H_E decreases for larger grain size [56,81,102,154,184,192,193]. It seems that, the role of the grain size is related not only to the change in its size, but also to the degree of texture, the spin structure and the AFM anisotropy.

6.3.4. Interface impurity layers

Finally, as expected, it was found that the presence of impurity layers (amorphous or oxidized layers and/or adsorbed C, H or H_2O) at the interface tend to decrease the magnitude of H_E [44, 84,89,158,276].

There exists a systematic study of this effect, where a metal layer of increasing thickness is deposited between the AFM and FM layers [118,119]. As was found for impurity layers, H_E decreases with the presence of the metal layer. However, H_E does not become zero after a few monolayers of the metal impurity layer, as expected for a pure interface phenomenon, but several nm of the impurity layer are needed to completely null-out H_E [118,119]. Unfortunately, the connection to the interfacial structure and uniformity of the interfacial layer has not been uniquely established.

6.4. Anisotropy

The simple intuitive models and the more sophisticated theories seem to agree that the exchange bias should be larger for larger AFM anisotropies [1,333,359–361]. There are a few studies attempting to address this question [93,115,195,196]. All investigations dealing with the role of the anisotropy seem to agree with the theories, however it is difficult to extract any quantitative conclusions from them. The main difficulty in analyzing these results rises from the fact that they involve mixtures or dilution of AFM materials [115,195,196], therefore the absolute value of the anisotropy is usually unknown. Moreover, it is important to consider that different materials have different blocking temperatures, thus H_E should be compared at the same reduced temperature T/T_B. Nevertheless, the comparisons of H_E between similar materials with different anisotropies (e.g. CoO–NiO, FeF_2–MnF_2) appear to differ somewhat from the $H_E \propto \sqrt{K_{AFM}}$

predictions of some theories [333,359–361]. However, since the anisotropy of the AFM material and H_E depend on the microstructure of the AFM layer, exact, quantitative analysis is difficult.

6.5. Blocking temperature

The exchange bias vanishes above a temperature often denoted as the 'blocking' temperature, T_B. In some cases T_B is much lower than the bulk T_N, however in other cases $T_B \approx T_N$ (see Tables 2–4). The origin of this effect seems to be related, at least in part, to the grain size and thickness of the AFM layer, through finite size effects [363]. In other words, if the grain size (or the layer thickness) is smaller (thinner) than a system dependent critical dimension of the AFM, the Néel temperature of the AFM is substantially reduced. This assumption seems to be supported by the fact that systems based on single crystal AFM and thick AFM films with large grains tend to have $T_B \approx T_N$ [12,72, 74,95,155], while systems with very thin films have $T_B < T_N$ [95,131,148,149,212].

Other size effects are caused by the fact that the anisotropy of the AFM depends on its dimensions and that the condition $K_{AFM}t_{AFM} > J_{INT}$ (Eq. (5)) has to be fulfilled [1]. Although the size effect on anisotropy has not been carefully studied, if we assume that the AFM anisotropy decreases as its size is reduced, a reduction of T_B would be expected. As discussed above smaller anisotropy implies smaller exchange bias and consequently $T_B < T_N$.

Other factors influencing T_B include stoichiometry [103] or presence of multiple phases [88] of certain thin film systems.

We have assumed so far the existence of a single, well defined T_B. However, due to the pervasive disorder such as different grain sizes or roughness inevitably there will be a distribution of blocking temperatures [64,88,171,194,198,224,241,242]. The T_B distribution can be studied by warming the sample to $T < T_B$ and then cooling it in the presence of a field opposite to the original cooling (growth) field. The change in exchange bias caused by these field coolings from different T ($T < T_B$), gives information about width of the T_B distribution [64,88,171,194,198,224,241,242].

6.6. Training effect

It is well known that in many exchange-biased film systems, H_E depends on the number of measurements, a property often called a *training effect* [45,58,80,86,103,123,126,188–190,192,195, 196,217,218,239,299]. For instance, if several consecutive hysteresis loops are measured, the shift (H_E) of consecutive loops will decrease. This phenomenon has also been observed using other techniques, such as torque measurements [190,218,239]. However, this effect is not observed in techniques which relay on small reversible movements of the magnetization [229–231]. It is often found experimentally that $H_E - H_{E\infty} \propto 1/\sqrt{n}$, where n indicates the order consecutive loops are measured (see Fig. 12) [218,239]. However, it is important to stress that this phenomenon is more important in polycrystalline AFM, and very small or non-existent in systems based on single crystals (bulk or thin films) [12,72,74,118,126].

This effect seems to be related to partial reorientation of the AFM domains with each FM magnetization reversal. The origin of this effect may lay on

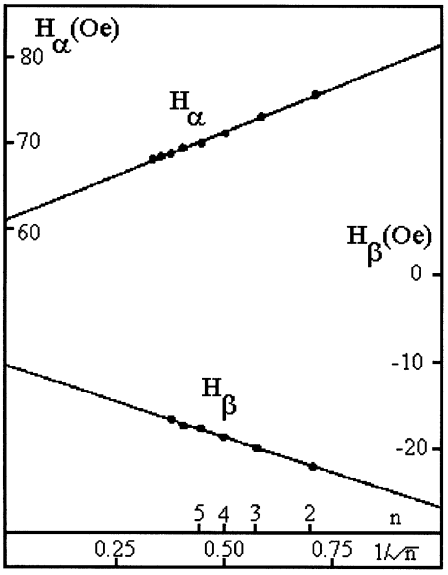

Fig. 12. Coercive fields for the increasing field branch, H_α, and decreasing field branch, H_β, of the hysteresis loop as a function of measurement order, n, for an $Fe_{20}Ni_{80}$/FeNiMn bilayer at room temperature [218].

a growth induced metastable spin configuration [359–361], an induced thermoremanent magnetization in the AFM layer, which exhibits some reptation effects [345–347], or caused by thermal fluctuations when $K_{AFM}t_{AFM} < k_BT$ [217]. The AFM spins try to find energetically favorable configurations after each cycle.

6.7. Coercivity

Although the coercivity, H_C, is strongly affected by the exchange anisotropy, it is seldom studied systematically. The coercivity usually increases below T_B, which is probably linked to the anisotropy of the AFM layer. Among comparable systems (e.g. similar FM and AFM thickness) containing similar AFM materials (e.g. NiO–CoO or FeF_2–MnF_2), those with smaller AFM anisotropy tend to have a larger increase in coercivity [93,115,195,196]. However, direct comparisons are difficult to carry out because the coercivity is also affected by the microstructure of the FM layer, which inevitably changes from system to system.

This increase in coercivity below T_B is intuitively simple to understand. In the case of an AFM with small anisotropy, when the FM rotates it 'drags' the AFM spins irreversibly, hence increasing the FM coercivity. For a large AFM anisotropy, the FM decouples because it cannot drag AFM spins, consequently the coercivity is reduced. A consequence of the influence of the anisotropy on the coercivity, is the peak which it often exhibits close to T_B [37,88,126,157,161,165,188,189], as shown in Fig. 13. This peak is due to the decrease of AFM anisotropy close to T_B. As the anisotropy decreases, the FM is able to drag increasingly more AFM spins, thus increasing the coercivity. Above T_B the AFM is random, thus it does not hinder the FM rotation. The width of the peak is related to sample homogeneity. In every sample, there is some spread on grain sizes, interface couplings, stress, and so on, which causes a distribution of AFM anisotropies. The distribution of AFM anisotropies reflects itself on the coercivity and therefore this peak mimics the sample inhomogeneity.

A similar peak behavior close to T_B has also been observed in the rotational hysteresis of some systems [52,131,217]. This indicates that the coercivity and the rotational hysteresis are different manifestations of the same effect, i.e. the losses produced during the rotation of the FM layer by the AFM spin drag [190].

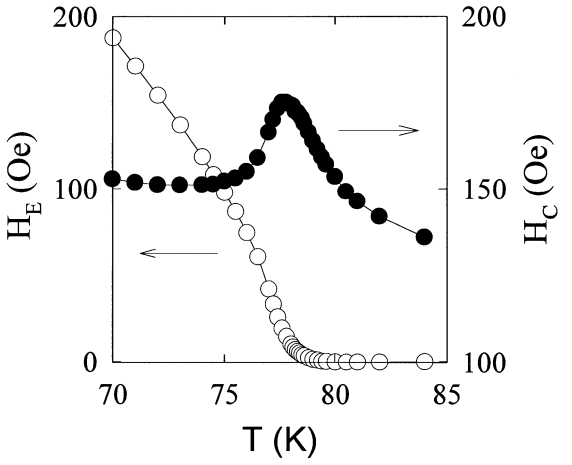

Fig. 13. Exchange bias, H_E, and coercivity, H_C, versus temperature for an FeF_2/Fe bilayer after field cooling.

As shown in Fig. 10, an analogous peak effect is found in the AFM thickness dependence of H_C [15,56,57,123,127,162,164,180,184,185,196,208,209] or the rotational hysteresis [131,210,212] at a fixed temperature. The explanation of this thickness dependent effect is similar to the previous temperature dependent one. In this case, as the AFM thickness decreases the effective AFM anisotropy, $K_{AFM}t_{AFM}$, is reduced. Thus, the FM can drag more AFM spins as the AFM layer is thinner, increasing the coercivity. For thin enough films, the AFM layer is no longer magnetic thus it stops hindering the FM rotation. However, one cannot rule out other pinning mechanisms, such as inhomogeneities in the AFM–FM coupling [180] or thermal fluctuations [344], as the source of these peak effects.

6.8. Cooling field – positive H_E

The effects of the cooling field amplitude (or the field applied during growth in some systems) are rarely reported [16,82,83]. This is probably because generally H_E does not depend markedly on cooling field. For example, for example, for FeMn/

$Fe_{20}Ni_{80}$, H_E is reduced by about 10% when cooled in 5 T instead of 300 Oe, as is often used [364]. However, studies in FeF_2/Fe and MnF_2/Fe bilayers revealed a rather unusual behavior [91,93]. The most striking result is that for large cooling fields the loops instead of shifting towards negative fields (for a positive cooling field), they shift to positive fields, i.e. in the same direction as the cooling field (Fig. 14) [91]. This is contrary to what is observed for small cooling field or what is observed in other systems [1–10]. This effect is often called *positive exchange bias* [91]. The magnitude of the cooling field needed to obtain a positive shift depends strongly on the microstructure of the sample, and thus the interface coupling at the interface. For strong couplings (i.e. large H_E at low cooling fields) larger cooling fields are needed to obtain positive loop shifts [91]. It is noteworthy that positive exchange has also been observed in FeF_2 single crystals coated with thin Fe layers for rather small cooling fields ($H_{COOL} = 2000$ Oe). This indicates that the interface coupling in this case is rather weak [72].

Different theoretical models have been proposed to explain this effect [91,350,362]. However, all the models are based on the existence of an *antiferromagnetic coupling* at the interface between the FM and AFM layers [91,350,362]. If the FM–AFM coupling is *ferromagnetic*, as usually assumed in most theoretical models, there should be no substantial effect of the cooling field [91,350,362].

6.9. Perpendicular coupling

In Section 5, we have stressed that most models assume collinear AFM–FM spins at the interface. However, it has been found experimentally that this is not necessarily true [71–73,101,209,217]. Several systems exhibit a *perpendicular coupling* at the interface between the FM and AFM spins: FeMn/$Fe_{20}Ni_{80}$ bilayers [209], CoO/Fe_3O_4 multilayers [101], CoO single crystals covered by an $Fe_{20}Ni_{80}$ film [71], FeF_2 (1 1 0) and FeF_2 (1 0 0) single crystals covered by Fe films [72,73]. Perpendicular coupling has been observed in compensated [72,73,101,209] and uncompensated [71–73] AFM surfaces. This effect has been theoretically predicted for AFM–FM systems when the FM has a low anistropy [362]. Moreover, some degree of non-collinear coupling has been observed in other systems by torque magnetometry [217] and domain observation [303,304].

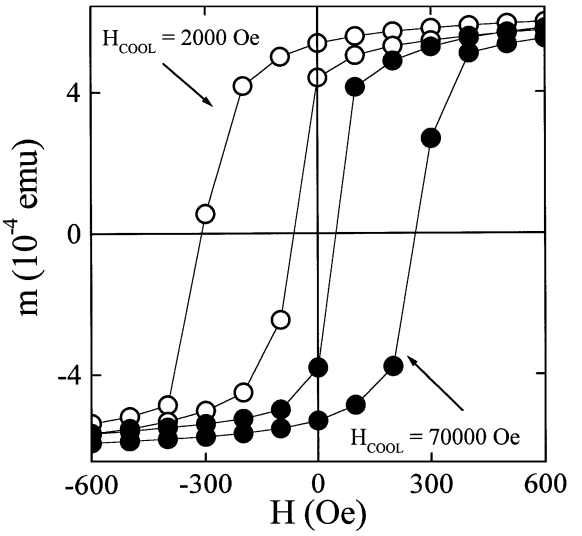

Fig. 14. Hysteresis loops, $m(H)$, for an FeF_2/Fe bilayer cooled in $H_{COOL} = 2000$ Oe (open symbols) and $H_{COOL} = 70\,000$ Oe (filled symbols), at $T = 10$ K [91].

The temperature dependence of FeF_2/Fe shows that the FM easy axis rotates 90° between room temperature and 10 K, with the rotation starting around the FeF_2 Néel temperature [72,73]. However, in CoO/Fe_3O_4 multilayers it is the AFM spins which appear to arrange perpendicular to the ferrimagnetic spins [101]. This indicates that as the AFM orders it is energetically advantageous for the FM–AFM spins to point in a perpendicular directions. Intuitively, the lowest energy configuration for a compensated surface is with the FM oriented perpendicular to the two AFM sublattices. This reasoning can be extended to uncompensated surfaces if due to fluctuations, e.g. roughness, domain formation, etc., the AFM spins arrange themselves antiparallel at the interface.

7. Conclusions

In conclusion, exchange bias, H_E, depends strongly on the spin structure at the interface. Both

intrinsic, e.g. spin orientation or anisotropy, and extrinsic, e.g. roughness or crystallinity, contribute to the magnitude of H_E. Consequently, the magnitude of H_E is a combination of many factors, which makes its theoretical analysis complicated.

From the applied point of view the main aims are to improve the layer quality to develop materials with large H_E, high T_B (well above room temperature), and good corrosion resistance. From the basic point of view, there is a need for studies aimed at understanding the interface spin structure, using novel tools such as circular magnetic dichroism or using conventional ones, such as neutron diffraction or Mössbauer spectroscopy, in unconventional ways. From the theoretical point of view, general models which include extrinsic and intrinsic phenomena and capable of explaining the new effects present (such as positive exchange bias or perpendicular coupling) are needed.

Despite the active research in this field, there are many factors influencing H_E which are poorly understood, including the role of AFM domains, AFM spin structure at the interface (e.g. orientations or interface disorder), the role of the AFM anisotropy or the perpendicular coupling at the interface.

Acknowledgements

We thank V. Speriosu for motivating our initial interest in exchange anisotropy. Discussions with D. Lederman, T.J. Moran, G.P. Felcher, M.R. Fitzsimmons, J.A. Borchers, Y. Ijiri, R.W. Erwin, R. Ramírez, M. Kiwi, G. Güntherodt, P. Miltényi, E.D. Dahlberg, K.V. Rao, Y.U. Idzerda, B.A. Gurney, A.E. Berkowitz, N.C. Koon, J. Mattinson, W.H. Meiklejohn and H. Suhl are greatly acknowledged. Special thanks to M. Kiwi and J.L. Vicent for critical reading of the manuscript. We wish to thank the authors who have made their articles available to us prior to publication. This work was supported by the U.S. Department of Energy and the UC-CULAR program. JN thanks the NATO Scientific Committee and the Spanish Ministerio de Educación y Ciencia for their financial support during his stay at UCSD. This review was completed on 20 December 1997.

References

[1] Review: W.H. Meiklejohn, J. Appl. Phys. 33 (1962) 1328.
[2] Review: C.P. Bean, in: C.A. Neugebauer, J.B. Newkirk, D.A. Vermilyea (Eds.), Structure and Properties of Thin Films, Wiley, New York, 1960, p. 331.
[3] W.H. Meiklejohn, C.P. Bean, Phys. Rev. 105 (1957) 904.
[4] Review: E.P. Wohlfarth, Adv. Phys. 8 (1959) 87.
[5] Review: H. Schmid, Cobalt 6 (1960) 8.
[6] Review: F.S. Luborsky, Electro-Technology (Sept. 1962) 107.
[7] Review: I.S. Jacobs, in: G.T. Rado, H. Suhl (Eds.), Magnetism, Academic Press, New York, 1963, p. 271.
[8] Review: J.S. Kouvel, J. Phys. Chem. Sol. 24 (1963) 795.
[9] Review: A. Yelon, in: M.H. Francombe, R.W. Hoffman (Eds.), Physics of Thin Films, vol. 6, Academic Press, New York, 1971, p. 205.
[10] Review: N.H. March, P. Lambin, F. Herman, J. Magn. Magn. Mater. 44 (1984) 1.
[11] W.H. Meiklejohn, C.P. Bean, Phys. Rev. 102 (1956) 1413.
[12] T.J. Moran, J.M. Gallego, I.K. Schuller, J. Appl. Phys. 78 (1995) 1887.
[13] A.E. Berkowitz, J.H. Greiner, J. Appl. Phys. 36 (1965) 3330.
[14] Review – AFM Properties: K. Fukamichi, J. Magn. Soc. Japan 21 (1997) 1062.
[15] R. Jungblut, R. Coehoorn, M.T. Johnson, J. aan de Stegge, A. Reinders, J. Appl. Phys. 75 (1994) 6659.
[16] M. Takahashi, A. Yanai, S. Taguchi, T. Suzuki, Jpn. J. Appl. Phys. 19 (1980) 1093.
[17] Review – Applications – GMR: J.C.S. Kools, IEEE Trans. Magn. 32 (1996) 3165.
[18] Review – Applications: C. Tang, J. Appl. Phys. 55 (1984) 2226.
[19] P.J. van der Zaag, R.M. Wolf, A.R. Ball, C. Bordel, L.F. Feiner, R. Jungblut, J. Magn. Magn. Mater. 148 (1995) 346.
[20] W.C. Cain, M.H. Kryder, J. Appl. Phys. 67 (1990) 5722.
[21] M. Ohkoshi, K. Tamari, M. Harada, S. Honda, T. Kusuda, IEEE Transl. J. Magn. Japan 1 (1985) 37.
[22] A.A. Glazer, A.P. Potapov, R.I. Tagirov, Sov. Phys. JETP. Lett. 15 (1972) 259.
[23] B. Dieny, V.S. Speriosu, S.S.P. Parkin, B.A. Gurney, D.R. Wilhoit, D. Mauri, Phys. Rev. B 43 (1991) 1297.
[24] M.N. Baibich, J.M. Broto, A. Fert, F. Nguyen Van Dau, F. Petroff, P. Etienne, G. Creuzet, A. Friederich, Phys. Rev. Lett. 61 (1988) 2472.
[25] P. Miltényi, M. Gruyters, J. Nogués, G. Güntherodt, I.K. Schuller, 1997, unpublished.
[26] D.S. Geoghegan, P.G. McCormick, R. Street, Mater. Sci. Forum 179–181 (1995) 629.
[27] F.J. Darnell, J. Appl. Phys. 32 (Suppl.) (1961) 186S.
[28] T. Iwata, K. Kai, T. Nakamichi, M. Yamamoto, J. Phys. Soc. Japan 28 (1970) 582.
[29] J.S. Kouvel, J. Phys. Chem. Sol. 21 (1961) 57.

[30] J.S. Kouvel, C.D. Graham Jr., J. Phys. Chem. Sol. 11 (1959) 220.
[31] A.A. Glazer, S.P. Potapov, Y.V. Belozerov, Phys. Met. Metall. 61 (1986) 54.
[32] G.L. Bona, F. Meier, H.C. Siegmann, R.J. Gambino, Appl. Phys. Lett. 52 (1988) 166.
[33] N. Sakamoto, J. Phys. Soc. Japan 17 (1962) 99.
[34] J. Bransky, I. Bransky, A.A. Hirsch, J. Appl. Phys. 41 (1970) 183.
[35] L. Smardz, U. Köbler, W. Zinn, Vacuum 42 (1991) 283.
[36] L. Smardz, U. Köbler, W. Zinn, J. Appl. Phys. 71 (1992) 5199.
[37] F.B. Hagedorn, J. Appl. Phys. 38 (1967) 3641.
[38] K. Tamari, A. Yamashita, M. Ohkoshi, S. Honda, T. Kusuda, IEEE Transl. J. Magn. Japan 1 (1985) 975.
[39] R.D. Hempstead, S. Krongelb, D.A. Thompson, IEEE Trans. Magn. 14 (1978) 521.
[40] W. Cao, G. Thomas, M.J. Carey, A.E. Berkowitz, J. Electron. Mater. 23 (1994) 1043.
[41] J. Fujikata, K. Hayashi, H. Yamamoto, K. Yamada, J. Magn. Soc. Japan 19 (1995) 365.
[42] K.T.Y. Kung, L.K. Louie, J. Appl. Phys. 69 (1991) 5634.
[43] M.M. Chen, C. Tsang, N. Gharsallah, IEEE Trans. Magn. 29 (1993) 4077.
[44] I. Yuitoo, M. Kitada, J. Jpn. Inst. Met. 57 (1993) 549.
[45] C. Tsang, K. Lee, J. Appl. Phys. 53 (1982) 2605.
[46] M.F. Toney, C. Tsang, J.K. Howard, J. Appl. Phys. 70 (1991) 6227.
[47] K. Nishioka, S. Gangopadhyay, A. Fujiwara, M. Parker, IEEE Trans. Magn. 32 (1995) 3949.
[48] A.J. Devasahayam, K.R. Mountfield, M.H. Kryder, IEEE Trans. Magn. 33 (1997) 2881.
[49] B.Y. Wong, C. Mitsumata, S. Prakash, D.E. Laughlin, T. Kobayashi, IEEE Trans. Magn. 32 (1996) 3425.
[50] B.Y. Wong, C. Mitsumata, S. Prakash, D.E. Laughlin, T. Kobayashi, J. Appl. Phys. 79 (1996) 7896.
[51] M. Tsunoda, M. Konoto, M. Takahashi, IEEE Trans. Magn. 33 (1997) 3688.
[52] J.H. Greiner, J. Appl. Phys. 37 (1966) 1474.
[53] P.P. Freitas, J.L. Leal, T.S. Plaskett, L.V. Melo, J.C. Soares, J. Appl. Phys. 75 (1994) 6480.
[54] V.A. Seredkin, G.I. Frolov, V.Y. Yakovchik, Phys. Met. Metall. 63 (1987) 34.
[55] V.A. Seredkin, G.I. Frolov, V.Y. Yakovchik, Sov. Tech. Phys. Lett. 9 (1983) 621.
[56] H. Uyama, Y. Otani, K. Fukamichi, O. Kitakami, Y. Shimada, J. Echigoya, Appl. Phys. Lett. 71 (1997) 1258.
[57] M. Takiguchi, N. Sugawara, A. Okabe, K. Hayashi, in: Digest of the 20th Conf. on Magnetics in Japan, Magn. Soc. Japan, 1996, p. 140.
[58] B. Kuhlow, M. Lambeck, H. Schroeder-Fürst, J. Wortmann, Z. Angew. Phys. 32 (1971) 54.
[59] M. Matsumoto, A. Morisako, S. Takei, S. Taijima, J. Magn. Soc. Japan 21 (1997) 509.
[60] K. Nishioka, C. Hou, H. Fujiwara, R.D. Metzger, J. Appl. Phys. 80 (1996) 4528.
[61] H.M. Lin, C.M. Hsu, Y.D. Yao, Y.Y. Chen, T.T. Kuan, F.A. Kuan, F.A. Yang, C.Y. Tung, NanoStruct. Mater. 6 (1995) 977.
[62] S. Gangopadhyay, G.C. Hadjipanayis, C.M. Sorensen, K.J. Klabunde, NanoStruct. Mater. 1 (1992) 449.
[63] S. Gangopadhyay, G.C. Hadjipanayis, C.M. Sorensen, K.J. Klabunde, J. Appl. Phys. 73 (1993) 6964.
[64] S. Gangopadhyay, G.C. Hadjipanayis, C.M. Sorensen, K.J. Klabunde, IEEE Trans. Magn. 28 (1992) 3174.
[65] J. Löffler, W. Wagner, H. van Swygenhoven, J. Meier, B. Doudin, J.P. Ansermet, Mater. Sci. Forum 235–238 (1997) 699; J. Löffler, H. van Swygenhoven, W. Wagner, J. Meier, B. Doubin, J.P. Ansermet, NanoStruct. Mater. 9 (1997) 523.
[66] V. Papaefthymiou, A. Kostikas, A. Simopulos, D. Niarchos, S. Gangopadhyay, G.C. Hadjipanayis, C.M. Sorensen, K.J. Klabunde, J. Appl. Phys. 67 (1990) 4487.
[67] W. Abdul-Razzaq, M. Wu, J. Appl. Phys. 69 (1991) 5078.
[68] R.B. Goldfarb, K.V. Rao, F.R. Fickett, H.S. Chen, J. Appl. Phys. 52 (1981) 1744.
[69] V. Korenivski, R.B. van Dover, Y. Suzuki, E.M. Gyorgy, J.M. Phillips, R.J. Felder, J. Appl. Phys. 79 (1996) 5926.
[70] Y. Suzuki, R.B. van Dover, E.M. Gyorgy, J.M. Phillips, V. Korenivski, D.J. Werder, C.H. Chen, R.J. Felder, R.J. Cava, J.J. Krajewski, W.F. Peck Jr., J. Appl. Phys. 79 (1996) 5923.
[71] T.J. Moran, I.K. Schuller, J. Appl. Phys. 79 (1996) 5109.
[72] J. Nogués, T.J. Moran, D. Lederman, I.K. Schuller, K.V. Rao, Phys. Rev. B (in press).
[73] T.J. Moran, J. Nogués, D. Lederman, I.K. Schuller, Appl. Phys. Lett. 72 (1998) 617.
[74] J. Nogués, D. Lederman, T.J. Moran, I.K. Schuller, K.V. Rao, Appl. Phys. Lett. 68 (1996) 3186.
[75] T.R. McGuire, T.S. Plaskett, R.J. Gambino, IEEE Trans. Magn. 29 (1993) 2714.
[76] X. Lin, G.C. Hadjipanayis, S.I. Shah, J. Appl. Phys. 75 (1994) 6676.
[77] X. Lin, A.S. Murthy, G.C. Hadjipanayis, C. Swann, S.I. Shah, J. Appl. Phys. 76 (1994) 6543.
[78] S. Spagna, R.E. Sager, M.B. Maple, Rev. Sci. Inst. 66 (1995) 5570.
[79] S. Spagna, M.B. Maple, R.E. Sager, J. Appl. Phys. 79 (1996) 4926.
[80] Y.J. Chen, D.K. Lottis, E.D. Dahlberg, J.N. Kuznia, A.M. Wowchak, P.I. Cohen, J. Appl. Phys. 69 (1991) 4523.
[81] C.M. Park, D.G. Hwang, S.S. Lee, K.A. Lee, in: Digest of INTERMAG, IEEE, New York, 1996, p. EA-10.
[82] C.M. Park, K.A. Lee, D.G. Hwang, S.S. Lee, M.Y. Kim, M.Y. Kim, J. Korean Phys. Soc. 31 (1997) 508.
[83] C.M. Park, D.G. Hwang, S.S. Lee, K.A. Lee, Ungyong Mulli 10 (1997) 221.
[84] M.A. Russak, S.M. Rossnagel, S.L. Cohen, T.R. McGuire, G.J. Scilla, C.V. Jahnes, J.M. Baker, J.J. Cuomo, J. Electrochem. Soc. 136 (1989) 1793.
[85] H. Fujiwara, K. Nishoka, C. Hou, M.R. Parker, S. Gangopadhyay, R. Metzger, J. Appl. Phys. 79 (1996) 6286.

[86] C. Schlenker, S.S.P. Parkin, J.C. Scott, K. Howard, J. Magn. Magn. Mater. 54–57 (1986) 801.
[87] R.D. McMichael, W.F. Egelhoff Jr., L.H. Bennet, IEEE Trans. Magn. 31 (1995) 3930.
[88] M. Tsunoda, Y. Tsuchiya, M. Konoto, M. Takahashi, J. Magn. Magn. Mater. 171 (1997) 29.
[89] K. Uneyama, M. Tsunoda, M. Konoto, M. Takahashi, J. Magn. Soc. Japan 21 (1997) 517.
[90] M. Tsunoda, M. Konoto, K. Uneyama, M. Takahashi, J. Magn. Soc. Japan 21 (1997) 513.
[91] J. Nogués, D. Lederman, T.J. Moran, I.K. Schuller, Phys. Rev. Lett. 76 (1996) 4624.
[92] D. Lederman, J. Nogués, I.K. Schuller, Phys. Rev. B 56 (1997) 2332.
[93] J. Nogués, I.K. Schuller, 1997, unpublished.
[94] D.V. Dimitrov, A.S. Murthy, G.C. Hadjipanayis, C.P. Swann, J. Appl. Phys. 79 (1996) 5106.
[95] P.J. van der Zaag, A.R. Ball, L.F. Feiner, R.M. Wolf, P.A.A. van der Heijden, J. Appl. Phys. 79 (1996) 5103.
[96] S.D. Berry, D.M. Lind, G. Chern, H. Mathias, J. Magn. Magn. Mater. 123 (1993) 126.
[97] S.D. Berry, D.M. Lind, E. Lochner, K.A. Shaw, D. Hilton, R.W. Erwin, J.A. Borchers, Mater. Res. Soc. Symp. Proc. 313 (1993) 779.
[98] D.M. Lind, S.P. Tay, S.D. Berry, J.A. Borchers, R.W. Erwin, J. Appl. Phys. 73 (1993) 6886.
[99] Y. Suzuki, R.B. van Dover, V. Korenivski, D. Werder, C.H. Chen, R.J. Felder, R.J. Cava, J.J. Krajewski, W.F. Peck Jr., Mater. Res. Soc. Symp. Proc. 401 (1996) 473.
[100] Y. Suzuki, R.B. van Dover, E.M. Gyorgy, J.M. Phillips, R.J. Felder, Phys. Rev. B 53 (1996) 14016.
[101] Y. Ijiri, J.A. Borchers, R.W. Erwin, S.H. Lee, P.J. van der Zaag, R.M. Wolf, Phys. Rev. Lett. 80 (1998) 608.
[102] K. Takano, R.H. Kodama, A.E. Berkowitz, W. Cao, G. Thomas, Phys. Rev. Lett. 79 (1997) 1130.
[103] Y. Tsuchiya, K. Kosuge, S. Yamaguchi, N. Nakayama, Mater. Trans. JIM 38 (1997) 91.
[104] R.H. Kodama, A.E. Berkowitz, E.J. McNiff, S. Foner, J. Appl. Phys. 81 (1997) 5552.
[105] R.H. Kodama, S.A. Makhlouf, A.E. Berkowitz, Phys. Rev. Lett. 79 (1997) 1393.
[106] R.F.C. Farrow, R.F. Marks, S. Gider, A.C. Marley, S.S.P. Parkin, J. Appl. Phys. 81 (1997) 4986.
[107] Y.D. Yao, Y.Y. Chen, C.M. Hsu, H.M. Lin, C.Y. Tung, M.F. Tai, D.H. Wang, K.T. Wu, C.T. Suo, NanoStruct. Mater. 6 (1995) 933.
[108] Y.D. Yao, Y.Y. Chen, M.F. Tai, D.H. Wang, H.M. Lin, Mater. Sci. Eng. A 217/218 (1996) 281.
[109] M.B. Stearns, J. Appl. Phys. 55 (1984) 1729.
[110] C.M. Hsu, H.M. Lin, K.R. Tsai, J. Appl. Phys. 76 (1994) 4793.
[111] N.N. Efimova, S.R. Kufterina, Y.A. Popkov, E.N. Khats'ko, A.S. Chernyi, Low Temp. Phys. 22 (1996) 824.
[112] Q.T. Wang, G.H. Pan, Y.X. Sun, J. Magn. Magn. Mater. 78 (1989) 190.
[113] K. Hemmes, T.J.A. Popma, J. Phys. D 21 (1988) 228.
[114] T. Tokunaga, M. Taguchi, T. Fukami, Y. Nakaki, K. Tsutsumi, J. Appl. Phys. 67 (1990) 4417.
[115] M.J. Carey, A.E. Berkowitz, Appl. Phys. Lett. 60 (1992) 3060.
[116] N. Oshima, M. Nakada, Y. Tsukamoto, Jpn. J. Appl. Phys. 33 (Part 2) (1996) L1585.
[117] K. O'Grady, S.J. Greaves, S.M. Thompson, J. Magn. Magn. Mater. 156 (1996) 253.
[118] N.J. Gökemeijer, T. Ambrose, C.L. Chien, N. Wang, K.K. Fung, J. Appl. Phys. 81 (1997) 4999.
[119] N.J. Gökemeijer, T. Ambrose, C.L. Chien, Phys. Rev. Lett. 79 (1997) 4270.
[120] S. Soeya, S. Tadokoro, T. Imagawa, M. Fuyama, J. Appl. Phys. 74 (1993) 6297.
[121] S.F. Cheng, J.P. Teter, P. Lubitz, M.M. Miller, L. Hoines, J.J. Krebs, D.M. Schaefer, G.A. Prinz, J. Appl. Phys. 79 (1996) 6234.
[122] J.X. Shen, M.T. Kief, J. Appl. Phys. 79 (1996) 5008.
[123] C.L. Lin, J.M. Sivertsen, J.H. Judy, IEEE Trans. Magn. 31 (1995) 4091.
[124] D.H. Han, J.G. Zhu, J.H. Judy, J. Appl. Phys. 81 (1997) 4996.
[125] D.H. Han, J.G. Zhu, J.H. Judy, J.M. Sivertsen, J. Appl. Phys. 81 (1997) 340.
[126] R.P. Michel, A. Chaiken, Y.K. Kim, L.E. Johnson, IEEE Trans. Magn. 32 (1996) 4651.
[127] T. Lin, C. Tsang, R.E. Fontana Jr., J.K. Howard, IEEE Trans. Magn. 31 (1995) 2584.
[128] S.X. Wang, W.E. Bailey, C. Sügers, IEEE Trans. Magn. 33 (1997) 2369.
[129] D.H. Han, J.G. Zhu, J.H. Judy, J.M. Sivertsen, J. Appl. Phys. 81 (1997) 4519.
[130] D.H. Han, J.G. Zhu, J.H. Judy, J.M. Sivertsen, Appl. Phys. Lett. 70 (1997) 664.
[131] S. Soeya, S. Nakamura, T. Iamgawa, S. Narishige, J. Appl. Phys. 77 (1995) 5838; S. Soeya, H. Hoshiya, K. Meguro, H. Fukui, Appl. Phys. Lett. 71 (1997) 3424.
[132] F. Koike, N. Hasegawa, A. Makino, J. Magn. Soc. Japan 20 (1996) 365.
[133] N. Hasegawa, A. Makino, F. Koike, K. Ikarashi, IEEE Trans. Magn. 32 (1996) 4618.
[134] M.J. Carey, A.E. Berkowitz, J. Appl. Phys. 73 (1993) 6892.
[135] J. Fujikata, K. Ishihara, K. Hayashi, H. Yamamoto, K. Yamada, IEEE Trans. Magn. 31 (1995) 3936.
[136] J. Fujikata, K. Hayashi, H. Yamamoto, M. Nakada, IEEE Trans. Magn. 32 (1996) 4621.
[137] A.A. Glazer, A.P. Potapov, R.I. Tagirov, Y.A. Shur, Phys. Stat. Sol. 16 (1966) 745.
[138] C.M. Park, K.I. Min, K.H. Shin, J. Appl. Phys. 79 (1996) 6228.
[139] H. Kanai, J. Kane, T. Yamamoto, J. Magn. Soc. Japan 20 (1996) 361.
[140] C. Tsang, N. Heiman, K. Lee, J. Appl. Phys. 52 (1981) 2471.
[141] G. Wang, T. Yeh, C.L. Lin, J.M. Sivertsen, J.H. Judy, IEEE Trans. Magn. 32 (1996) 4660.
[142] J.K. Howard, T.C. Huang, J. Appl. Phys. 64 (1988) 6118.

[143] Y.K. Kim, K. Ha, L.L. Rea, IEEE Trans. Magn. 31 (1995) 3823.
[144] R. Nakatani, H. Hoshiya, K. Hoshino, Y. Sugita, IEEE Trans. Magn. 33 (1997) 3682.
[145] R. Nakatani, H. Hoshiya, K. Hoshino, Y. Sugita, J. Magn. Magn. Mater. 173 (1997) 321.
[146] H. Iwasaki, A.T. Saito, A. Tsutai, M. Sahashi, IEEE Trans. Magn. 33 (1997) 2875.
[147] A.M. Goodman, K. O'Grady, N.S. Walmsley, M.R. Parker, IEEE Trans. Magn. 33 (1997) 2902.
[148] S.S.P. Parkin, V.S. Speriosu, in: L.M. Falicov, F. Mejía-Lira, J.L. Morán-López (Eds.), Magnetic Properties of Low-Dimensional Systems II, Springer, Berlin, 1990, p. 110.
[149] K. Hoshino, S. Noguchi, R. Nakatani, H. Hoshiya, Y. Sugita, Jpn. J. Appl. Phys. 33 (1994) 1327.
[150] Y. Miyamoto, T. Yoshitani, S. Nakagawa, M. Naoe, IEEE Trans. Magn. 32 (1997) 4672.
[151] R. Nakatani, K. Hoshino, Y. Sugita, Mater. Trans. JIM 37 (1996) 1458.
[152] M. Fujita, K. Yamano, A. Maeda, T. Tanuma, M. Kume, J. Appl. Phys. 81 (1997) 4909.
[153] R. Nakatani, K. Hoshino, S. Noguchia, Y. Sugita, Jpn. J. Appl. Phys. 33 (1994) 133.
[154] T. Umemoto, A. Maeda, S. Takahashi, T. Tanuma, M. Kume, Jpn. J. Appl. Phys. 36 (1997) 6746.
[155] G. Choe, S. Gupta, Appl. Phys. Lett. 70 (1997) 1766.
[156] H. Kishi, Y. Kitade, Y. Miyake, A. Tanaka, K. Kobayashi, IEEE Trans. Magn. 32 (1996) 3380.
[157] H. Kishi, Y. Shimizu, K. Nagasaka, A. Tanaka, M. Oshiki, J. Magn. Soc. Japan 21 (1997) 521.
[158] K. Uneyama, M. Tsunoda, M. Takahashi, IEEE Trans. Magn. 33 (1997) 3685.
[159] M. Tsunoda, Y. Tsuchiya, M. Takahashi, T. Wakiyama, J. Magn. Soc. Japan 20 (1996) 393.
[160] T. Lin, G.L. Gorman, C. Tsang, IEEE Trans. Magn. 32 (1996) 3443.
[161] A.J. Devasahayam, M.H. Kryder, IEEE Trans. Magn. 32 (1996) 4654.
[162] T.J. Klemmer, V.R. Inturi, M.K. Minor, J.A. Barnard, Appl. Phys. Lett. 70 (1997) 2915.
[163] T. Lin, D. Mauri, N. Staud, C. Hwang, J.K. Howard, Appl. Phys. Lett. 65 (1994) 1183.
[164] H. Hoshiya, S. Soeya, Y. Hamakawa, R. Nakatani, IEEE Trans. Magn. 33 (1997) 2878.
[165] M. Saito, Y. Kakaihara, T. Watanabe, N. Hasegawa, J. Magn. Soc. Japan 21 (1997) 505.
[166] F. Hellman, R.B. van Dover, E.M. Gyorgy, Appl. Phys. Lett. 50 (1987) 296.
[167] T. Terashima, Y. Bando, Thin Solid Films 152 (1987) 455.
[168] S. Mao, S. Gangopadhyay, N. Amin, E. Murdock, Appl. Phys. Lett. 69 (1996) 3593.
[169] T. Ambrose, R.L. Sommer, C.L. Chien, Phys. Rev. B 56 (1997) 83.
[170] T. Ataka, K. Ohkubo, N. Nagano, N. Sawatari, K. Matsuzaki, in: Digest of the 17th Conf. on Magnetics in Japan, Magn. Soc. Japan, 1993, p. 35.
[171] Y. Tsuchiya, Rec. Elec. Commun. Eng. Conver. Tohoku Univ. 65 (1996) 153.
[172] T. Ambrose, C.L. Chien, Appl. Phys. Lett. 65 (1994) 1967.
[173] T. Ambrose, K. Leifer, K.J. Hemker, C.L. Chien, J. Appl. Phys. 81 (1997) 5007.
[174] K. Hoshino, R. Nakatani, H. Hoshiya, Y. Sugita, S. Tsunashima, Jpn. J. Appl. Phys. 35 (1996) 607.
[175] A.M. Choukh, IEEE Trans. Magn. 33 (1997) 3676.
[176] G. Choe, S. Gupta, IEEE Trans. Magn. 33 (1997) 3691.
[177] A. Tanaka, Y. Shimizu, H. Kishi, K. Nagasaka, M. Oshiki, IEEE Trans. Magn. 33 (1997) 3592.
[178] X. Portier, A.K. Petford-Long, T.C. Anthony, IEEE Trans. Magn. 33 (1997) 3679.
[179] H.C. Tong, M. Lederman, W. Jensen, M. Tan, D. Ravipati, S. Yuan, P. Thayamballi, D. Wagner, B. Huang, M. Zhao, P. Rana, W. Chen, L. Miloslavsky, D. O'Kane, R. Rottmayer, M. Dugas, IEEE Trans. Magn. 33 (1997) 2884.
[180] O. Kitakami, H. Takashima, Y. Shimada, J. Magn. Magn. Mater. 164 (1996) 43.
[181] X. Lin, J.G. Zhu, G. Wang, IEEE Trans. Magn. 33 (1997) 3987.
[182] J.G. Zhu, Y. Zheng, X. Lin, J. Appl. Phys. 81 (1997) 4336.
[183] H.N. Fuke, K. Saito, Y. Kamiguchi, H. Iwasaki, M. Sahashi, J. Appl. Phys. 81 (1997) 4004.
[184] H. Uyama, Y. Otani, K. Fukamichi, O. Kitakami, Y. Shimada, J. Echigoya, J. Magn. Soc. Japan 21 (1997) 911.
[185] S. Tanoue, J. Magn. Soc. Japan 21 (1997) 529.
[186] C. Schlenker, R. Buder, Czech. J. Phys. B 21 (1971) 506.
[187] C. Schlenker, R. Buder, Phys. Stat. Sol. A 4 (1971) K79.
[188] E. Fulcomer, S.H. Charap, J. Appl. Phys. 43 (1972) 4184.
[189] S.H. Charp, E. Fulcomer, J. Appl. Phys. 42 (1971) 1426.
[190] D. Paccard, C. Schlenker, O. Massanet, R. Montmory, A. Yelon, Phys. Stat. Sol. 16 (1966) 301.
[191] A.G. Zvegintsev, A.Y. Vlasov, N.A. Chetvergov, Sov. Phys. J. 6 (1969) 16.
[192] C.H. Lai, T.C. Anthony, R. Iwamura, R.L. White, IEEE Trans. Magn. 32 (1996) 3419.
[193] C.H. Lai, H. Matsuyama, R.L. White, T.C. Anthony, IEEE Trans. Magn. 31 (1995) 2609.
[194] C.H. Lai, T.J. Regan, R.L. White, T.C. Anthony, J. Appl. Phys. 81 (1997) 3989.
[195] C.H. Lai, W.E. Bailey, R.L. White, T.C. Anthony, J. Appl. Phys. 81 (1997) 4990.
[196] C.H. Lai, H. Matsuyama, R.L. White, T.C. Anthony, G.G. Bush, J. Appl. Phys. 79 (1996) 6389.
[197] S. Soeya, M. Fuyama, S. Tadokoro, T. Imagawa, J. Appl. Phys. 79 (1996) 1604.
[198] S. Soeya, T. Imagawa, K. Mitsuoka, S. Narishige, J. Appl. Phys. 76 (1994) 5356.
[199] D. Guarisco, E. Kay, S.X. Wang, IEEE Trans. Magn. 33 (1997) 3595.
[200] O. Massanet, R. Montmory, C. R. Acad. Sci. Paris 258 (1964) 1752.
[201] O. Massanet, R. Montmory, L. Néel, IEEE Trans. Magn. 1 (1965) 63.

[202] A.A. Glazer, A.P. Potapov, R.I. Tagirov, L.D. Uryasheva, Y.S. Shur, Bull. Acad. Sci. USSR Phys. Ser. 31 (1967) 738.
[203] A.A. Glazer, A.P. Potapov, R.I. Tagirov, Y.S. Shur, Sov. Phys. Sol. State 8 (1967) 2413.
[204] A.A. Glazer, R.I. Tagirov, A.P. Potapov, Y.S. Shur, Phys. Met. Metall. 26 (1968) 289.
[205] A.A. Glazer, Phys. Met. Metall. 30 (1970) 226.
[206] A.S. Yerukhimov, V.A. Seredkin, V.Y. Yakovchuk, Phys. Met. Metall. 52 (1981) 45.
[207] M.S. Yerukhimov, V.A. Seredkin, Phys. Met. Metall. 44 (1977) 70.
[208] D. Mauri, E. Kay, D. Scholl, J.K. Howard, J. Appl. Phys. 62 (1987) 2929.
[209] R. Jungblut, R. Coehoorn, M.T. Johnson, C. Sauer, P.J. van der Zaag, A.R. Ball, T.G.S.M. Rijks, J. aan de Stegge, A. Reinders, J. Magn. Magn. Mater. 148 (1995) 300.
[210] S. Tadokoro, T. Imagawa, M. Mitsuoka, S. Narishige, S. Soeya, M. Fuyama, J. Magn. Soc. Japan 20 (1996) 357.
[211] S. Soeya, H. Hoshiya, R. Arai, M. Fuyama, J. Appl. Phys. 81 (1997) 6488.
[212] S. Soeya, H. Hoshiya, M. Fuyama, J. Appl. Phys. 80 (1996) 1006.
[213] A. Berger, H. Hopster, Phys. Rev. Lett. 73 (1994) 193.
[214] Y. Fujii, T. Tokunaga, K. Hashima, K. Tsutsumi, H. Sugahara, J. Magn. Soc. Japan 11 (Suppl. S1) (1987) 329.
[215] K. Watanabe, S. Tadokoro, T. Kawabe, M. Fuyama, H. Fukui, S. Narishige, J. Magn. Soc. Japan 18 (Suppl. S1) (1994) 355.
[216] H. Danan, H. Gengnagel, J. Steinert, A. Linzen, J. de Phys. (France) Coll. 32 (1971) C1-131.
[217] C. Schlenker, Phys. Stat. Sol. 28 (1968) 507.
[218] C. Schlenker, D. Paccard, J. de Phys. (France) 28 (1967) 611.
[219] W.C. Cain, W.H. Meiklejohn, M.H. Kryder, J. Appl. Phys. 61 (1987) 4170.
[220] M. Tan, H.C. Tong, S.I. Tan, R. Rottmayer, J. Appl. Phys. 79 (1996) 5021.
[221] A.J. Devasahayam, M.H. Kryder, IEEE Trans. Magn. 31 (1995) 3820.
[222] C. Hwang, M.A. Parker, J.K. Howard, Mater. Res. Soc. Symp. Proc. 232 (1991) 217.
[223] O. Allegranza, M.M. Chen, J. Appl. Phys. 73 (1993) 6218.
[224] H. Fujimori, X. Lin, H. Morita, J. de Phys. (France) Coll. 49 (1988) C8-1931.
[225] W.E. Bailey, N.C. Zhu, R. Sinclair, S.X. Wang, J. Appl. Phys. 79 (1996) 6393.
[226] R.W. Sharp, P.C. Archibald, J. Appl. Phys. 37 (1966) 1462.
[227] S.B. Bailey, T.M. Peterlin, R.T. Richard, E.N. Mitchell, J. Appl. Phys. 41 (1970) 194.
[228] M.J. Pechan, I.K. Schuller, Phys. Rev. Lett. 59 (1987) 132.
[229] B.H. Miller, E.D. Dahlberg, Appl. Phys. Lett. 69 (1996) 3932.
[230] B.H. Miller, E.D. Dahlberg, J. Appl. Phys. 81 (1997) 5002.
[231] V. Ström, B.J. Jönsson, K.V. Rao, E.D. Dahlberg, J. Appl. Phys. 81 (1997) 5003.
[232] P. Miltényi, M. Gruyters, G. Güntherodt, J. Nogués, I.K. Schuller, Phys. Rev. B, in press.
[233] H. Heffner, G. Wade, J. Appl. Phys. 31 (1960) 2316.
[234] J.H. Greiner, I.M. Croll, M. Sulich, J. Appl. Phys. 32 (Suppl.) (1961) 188S.
[235] I.A. Campbell, H. Hurdequint, F. Hippert, Phys. Rev. B 33 (1986) 3540.
[236] H. Morita, H. Hiroyoshi, K. Fukamichi, J. Phys. F 16 (1986) 507.
[237] E.V. Shipil', K.Y. Guslienko, B. Szymanski, IEEE Trans. Magn. 30 (1994) 797.
[238] A.E. Berkowitz, J.H. Greiner, J. Appl. Phys. 35 (1964) 925.
[239] C. Schlenker, J. de Phys. (France) Coll. 29 (1968) C2-157.
[240] J.M. Lommel, C.D. Graham Jr., J. Appl. Phys. 33 (Suppl.) (1962) 1160.
[241] V.S. Speriosu, D.A. Herman Jr., I.L. Sanders, T. Yogi, IBM J. Res. Dev. 34 (1990) 884.
[242] V.S. Speriosu, S.S.P. Parkin, in: Digest of the Magnetic Recording Conf., IEEE, New York, 1990.
[243] W.H. Meiklejohn, J. Appl. Phys. 29 (1958) 454.
[244] B. Aktas, Y. Öner, H.Z. Durusoy, J. Magn. Magn. Mater. 119 (1993) 339.
[245] K. Tagaya, M. Fukada, J. Phys. Soc. Japan 46 (1979) 53.
[246] M.M.P. Janssen, J. Appl. Phys. 41 (1970) 399.
[247] A. Layadi, W.C. Cain, J.W. Lee, J.O. Artman, IEEE Trans. Magn. 23 (1987) 2993.
[248] N.M. Salansky, B.P. Khrustalev, A.A. Glazer, A.S. Melnik, Z.I. Sinegubova, Sov. Phys. JETP 30 (1970) 823.
[249] N.M. Salansky, B.P. Khrustalev, A.S. Melnik, L.A. Slanskaya, Z.I. Sinegubova, Thin Solid Films 4 (1969) 105.
[250] N.M. Salansky, B.P. Khrustalev, A.S. Melnik, Sov. Phys. JETP 29 (1969) 238.
[251] Y.V. Zakharov, B.P. Khrustalev, E.A. Khlebopros, A.S. Melnik, Sov. Phys. Sol. State 25 (1983) 1928.
[252] B. Waksmann, R. Buder, P. Escudier, C.F. Kooi, O. Massanet, J. de Phys. (France) Coll. 29 (1968) C2-128.
[253] B. Waksmann, O. Massanet, P. Escudier, C.F. Kooi, J. Appl. Phys. 39 (1968) 1389.
[254] B.P. Khrustalev, A.S. Mel'nik, Phys. Met. Metall. 36 (1973) 204.
[255] W. Stoecklein, S.S.P. Parkin, J.C. Scott, Phys. Rev. B 38 (1988) 6847.
[256] J.C. Scott, J. Appl. Phys. 57 (1985) 3681.
[257] V.S. Speriosu, S.S.P. Parkin, C.H. Wilts, IEEE Trans. Magn. 23 (1987) 2999.
[258] A. Layadi, J.W. Lee, J.O. Artman, J. Appl. Phys. 63 (1988) 3808.
[259] A. Layadi, J.W. Lee, J.O. Artman, J. Appl. Phys. 64 (1988) 6101.
[260] C.F. Kooi, W.R. Holmquist, P.E. Wigen, J.T. Doherty, J. Phys. Soc. Japan 17 (Suppl. B-I) (1962) 599.
[261] G.P. Felcher, Y.Y. Huang, M. Carey, A.E. Berkowitz, J. Magn. Magn. Mater. 121 (1993) 105.
[262] S.S.P. Parkin, V.P. Deline, R.O. Hilleke, G.P. Felcher, Phys. Rev. B 42 (1990) 10538.
[263] S.J. Blundell, J.A.C. Bland, Phys. Rev. B 46 (1992) 3391.

[264] A.R. Ball, H. Fredrikze, P.J. van der Zaag, R. Jungblut, A. Reinders, A. van der Graaf, M.T. Rekveldt, J. Magn. Magn. Mater. 148 (1995) 46.
[265] A.R. Ball, H. Fredrikze, D.M. Lind, R.M. Wolf, P.J.H. Bloemen, M.T. Rekveldt, P.J. van der Zaag, Physica B 211 (1996) 388.
[266] A.R. Ball, A.J.G. Leenaers, P.J. van der Zaag, K.A. Shaw, B. Singer, D.M. Lind, H. Fredrikze, M.T. Rekveldt, Appl. Phys. Lett. 69 (1996) 583.
[267] A.R. Ball, A.J.G. Leenaers, P.J. van der Zaag, K.A. Shaw, B. Singer, D.M. Lind, H. Fredrikze, M.T. Rekveldt, Appl. Phys. Lett. 69 (1996) 1489.
[268] J.A. Borchers, R.W. Erwin, S.D. Berry, D.M. Lind, J.F. Ankner, E. Lochner, K.A. Shaw, D. Hilton, Phys. Rev. B 51 (1995) 8276.
[269] D.M. Lind, J.A. Borchers, R.W. Erwin, J.F. Ankner, E. Lochner, K.A. Shaw, R.C. DiBari, W. Portwine, P. Stoyonov, S.D. Berry, J. Appl. Phys. 76 (1994) 6284.
[270] A. van der Graaf, A.R. Ball, J.C.S. Kools, J. Magn. Magn. Mater. 165 (1997) 479.
[271] B.A. Everitt, D. Wang, J.M. Daughton, IEEE Trans. Magn. 32 (1996) 4657.
[272] K. Nakamoto, Y. Kawato, Y. Suzuki, Y. Hamakawa, T. Kawabe, K. Fujimoto, M. Fuyama, Y. Sugita, IEEE Trans. Magn. 32 (1996) 3374.
[273] S.S. Lee, D.G. Hwang, C.M. Park, K.A. Lee, J.R. Rhee, J. Appl. Phys. 81 (1997) 5298.
[274] S.L. Burkett, S. Kora, J.L. Bresowar, J.C. Lusth, B.H. Pirkle, M.R. Parker, J. Appl. Phys. 81 (1997) 4912.
[275] S.S. Lee, D.G. Hwang, C.M. Park, K.A. Lee, IEEE Trans. Magn. 33 (1997) 3547.
[276] H.S. Chopra, B.J. Hockey, P.J. Chen, R.D. McMichael, W.F. Egelhoff Jr., J. Appl. Phys. 81 (1997) 4017.
[277] W.F. Egelhoff Jr., P.J. Chen, C.J. Powell, M. Stiles, R.D. McMichael, J. Appl. Phys. 79 (1996) 2491.
[278] K.M.H. Lenssen, A.E.M. de Vierman, J.J.T.M. Donkers, J. Appl. Phys. 81 (1997) 4915.
[279] S.L. Burkett, S. Kora, J.C. Lusth, IEEE Trans. Magn. 33 (1997) 3544.
[280] P. Bayle-Guillemaud, A.K. Petford-Long, T.C. Anthony, J.A. Burg, IEEE Trans. Magn. 32 (1996) 4627.
[281] M.F. Gillies, J.N. Chapman, J.C.S. Kools, J. Appl. Phys. 78 (1995) 5554.
[282] N. Smith, A.M. Zeltser, D.L. Yang, P.V. Koeppe, IEEE Trans. Magn. 33 (1997) 3385.
[283] H. Yoda, H. Iwasaki, T. Kobayashi, A. Tsutai, M. Sahashi, IEEE Trans. Magn. 32 (1996) 3363.
[284] M. Saito, Y. Kakihara, T. Watanabe, F. Koike, H. Seki, N. Hasegawa, K. Sato, T. Kuriyama, J. Magn. Soc. Japan 21 (1997) 525.
[285] J.L. Leal, N.J. Oliveira, L.M. Rodrigues, A.T. Sousa, P.P. Freitas, IEEE Trans. Magn. 30 (1994) 3831.
[286] P.P. Freitas, J.L. Leal, L.V. Melo, N.J. Oliveira, L. Rodrigues, A.T. Sousa, Appl. Phys. Lett. 65 (1994) 493.
[287] N.J. Oliveira, J.L. Ferreira, J. Pinheiro, A.M. Fernandes, O. Redon, S.X. Li, P. ten Berge, T.S. Plaskett, P.P. Freitas, J. Appl. Phys. 81 (1997) 4903.
[288] Y. Hamakawa, H. Hoshiya, T. Kawabe, Y. Suzuki, R. Arai, K. Nakamoto, M. Fuyama, Y. Sugita, IEEE Trans. Magn. 32 (1996) 149.
[289] S.L. Burkett, J.C. Lusth, J.L. Bresowar, M.R. Parker, J. Magn. Magn. Mater. 168 (1997) L233.
[290] R.D. McMichael, P.J. Chen, W.F. Egelhoff Jr., IEEE Trans. Magn. 33 (1997) 3589.
[291] L. Tang, D.E. Laughlin, S. Gangopadhyay, J. Appl. Phys. 81 (1997) 4906.
[292] S. Kumagai, N. Tezuka, T. Miyazaki, Jpn. J. Appl. Phys. 36 (1997) 1498.
[293] K. Ikarashi, N. Hasegawa, A. Makino, in: Digest of the 20th Conf. on Magnetics in Japan, Magn. Soc. Japan, 1996, p. 275.
[294] Y. Chen, D.K. Lottis, E.D. Dahlberg, J. Appl. Phys. 70 (1991) 5822.
[295] Y. Chen, D.K. Lottis, E.D. Dahlberg, Mod. Phys. Lett. 5 (1991) 1781.
[296] H. Roux-Buisson, J.C. Bruyere, Czech J. Phys. B 21 (1971) 516.
[297] R. Gontarz, H. Ratajczak, Z. Sczaniecki, Czech. J. Phys. B 21 (1971) 519.
[298] G.I. Frolov, A.A. Glazer, N.M. Salansky, V.N. Krotenko, Phys. Met. Metall. 28 (1969) 777.
[299] B. Kuhlow, M. Lambeck, H. Schroeder-Fürst, J. Wortman, Phys. Lett. A 34 (1971) 223.
[300] A.A. Glazer, A.P. Potapov, R.I. Tagirov, Bull. Acad. Sci. USSR Phys. Ser. 30 (1966) 1105.
[301] W. Rave, W.C. Cain, A. Hubert, M. Kryder, IEEE Trans. Magn. 23 (1987) 2164.
[302] J.N. Chapman, M.F. Gilles, P.P. Freitas, J. Appl. Phys. 79 (1996) 6452.
[303] O. Bostanjoglo, P. Kreisel, Phys. Stat. Sol. A 7 (1971) 173.
[304] O. Bostanjoglo, W. Giese, Int. J. Magn. 3 (1972) 135.
[305] V.S. Gornakov, V.I. Nikitenko, L.H. Bennett, H.J. Brown, M.J. Donahue, W.F. Egelhoff Jr., R.D. McMichael, A.J. Shapiro, J. Appl. Phys. 81 (1997) 5215.
[306] H.S. Chopra, B.J. Hockey, L.J. Swartzendruber, S.Z. Hua, P.J. Chen, D.S. Lashmore, M. Wuttig, W.F. Egelhoff Jr., NanoStruct. Mater. 9 (1997) 451.
[307] Y. Iwasaki, M. Takiguchi, K. Bessho, J. Appl. Phys. 81 (1997) 5021.
[308] J. Ding, J.G. Zhu, J. Appl. Phys. 79 (1996) 5892.
[309] A. Ercole, T. Fujimoto, M. Patel, C. Daboo, R.J. Hicken, J.A.C. Bland, J. Magn. Magn. Mater. 156 (1996) 121.
[310] J.W. Freeland, J. Nogués, Y.U. Idzerda, I.K. Schuller, 1997, unpublished.
[311] K. Takano, F.T. Parker, A.E. Berkowitz, J. Appl. Phys. 81 (1997) 5262.
[312] Review – Spin Glass: P.A. Beck, Prog. Mater. Sci. 23 (1978) 1.
[313] Review – Spin Glass: J.A. Mydosh, AIP Conf. Proc. 24 (1975) 131.
[314] J.S. Kouvel, W. Abdul-Razzaq, J. Magn. Magn. Mater. 53 (1985) 139.
[315] N. Smith, W.C. Cain, J. Appl. Phys. 69 (1991) 2471.

[316] Review – Applications – GMR: D.E. Heim, R.E. Fontana Jr., C. Tsang, V.S. Speriosu, B.A. Gurney, M.L. Williams, IEEE Trans. Magn. 30 (1994) 216.
[317] Review – Applications – GMR: J.M. Daughton, Y.J. Chen, IEEE Trans. Magn. 29 (1993) 2705.
[318] Review – Applications – GMR: B.A. Gurney, V.S. Speriosu, D.R. Wilhoit, H. Lefakis, R.E. Fontana Jr., D.E. Heim, M. Dovek, J. Appl. Phys. 81 (1997) 3998.
[319] Review – Applications – GMR: K.M.H. Lenssen, H.W. van Kestern, T.G.S.M. Rijks, J.C.S. Kools, M.C. de Nooijer, R. Coehoorn, W. Folkerts, Sensors and Actuators A 60 (1997) 90.
[320] N.M. Salansky, V.A. Seredkin, V.A. Burmakin, A.V. Nabatov, Sov. Phys. JETP 38 (1974) 1011.
[321] Review – Applications: C. Tsang, M.M. Chen, T. Yogi, Proc. IEEE 81 (1993) 1344.
[322] W.C. Cain, M.H. Kryder, IEEE Trans. Magn. 26 (1990) 2412.
[323] C. Tsang, R.E. Fontana Jr., IEEE Trans. Magn. 18 (1982) 1149.
[324] C. Tsang, IEEE Trans. Magn. 25 (1989) 3692.
[325] N. Miyamoto, N. Koyama, K. Mitsuoka, H. Fukui, J. Magn. Soc. Japan 19 (1995) 105.
[326] Review – GMR: B. Dieny, J. Magn. Magn. Mater. 136 (1994) 335.
[327] M.M. Miller, G.A. Prinz, P. Lubitz, L. Hoines, J.J. Krebs, S.F. Cheng, F.G. Parsons, J. Appl. Phys. 81 (1997) 4284.
[328] M.M. Miller, P. Lubitz, G.A. Prinz, J.J. Krebs, A.S. Edelstein, S.F. Cheng, F.G. Parsons, IEEE Trans. Magn. 33 (1997) 3388.
[329] L.V. Melo, L.M. Rodrigues, P.P. Freitas, IEEE Trans. Magn. 33 (1997) 3295.
[330] K. Matsuyama, H. Asada, S. Ikeda, K. Taniguchi, IEEE Trans. Magn. 33 (1997) 3283.
[331] D.D. Tang, P.K. Wang, V.S. Speriosu, S. Le, K.K. Kung, IEEE Trans. Magn. 31 (1995) 3206.
[332] W.C. Cain, M.H. Kryder, IEEE Trans. Magn. 25 (1989) 2787.
[333] D. Mauri, H.C. Siegmann, P.S. Bagus, E. Kay, J. Appl. Phys. 62 (1987) 3047.
[334] A. Aharoni, E.H. Frei, S. Shtrikman, J. Appl. Phys. 30 (1959) 1956.
[335] E. Goto, N. Hayashi, T. Miyashita, K. Nakagawa, J. Appl. Phys. 36 (1965) 2951.
[336] F.B. Hagedorn, J. Appl. Phys. 41 (1970) 2491.
[337] N.M. Salansky, E.G. Khasanov, K.M. Mukimov, Sov. Phys. Solid State 17 (1976) 1865.
[338] Y.V. Zakharov, V.A. Ignatchenko, Sov. Phys. JETP 32 (1971) 517.
[339] Y.V. Zakharov, E.A. Khlebopros, Sov. Phys. Solid State 22 (1980) 2137.
[340] A.V. Zuyev, D.I. Sementsov, Phys. Met. Metall. 42 (1976) 32.
[341] K.B. Vlasov, N.V. Volkenshtein, S.V. Vonosovskii, A.I. Mitsek, M.I. Turchinskaya, Bull. Acad. USSR Phys. Ser. 28 (1964) 338.
[342] K.B. Vlasov, A. Mishchek, Phys. Met. Metall. 14 (1962) 487.
[343] K.B. Vlasov, A. Mishchek, Phys. Met. Metall. 14 (1962) 498.
[344] E. Fulcomer, S.H. Charp, J. Appl. Phys. 43 (1972) 4190.
[345] L. Néel, Ann. Phys. (France) 1 (1967) 61.
[346] N. Kurti (Ed.), Selected Works of Louis Néel, Gordon and Breach, New York, 1988.
[347] L. Néel, C.R. Acad. Sci. Paris Serie C 264 (1967) 1002.
[348] Y.S. Sanoyan, K.A. Yegiyan, Phys. Met. Metall. 38 (1974) 231.
[349] W. Brodkorb, W. Haubenreisser, Phys. Stat. Sol. A 3 (1970) 333.
[350] R. Ramírez, M. Kiwi, D. Lederman, Bull. Am. Phys. Soc. 42 (1997) 445.
[351] M.G. Mal'bin, V.I. Saprykin, Phys. Met. Metall. 38 (1974) 63.
[352] N.M. Salansky, M.S. Eruchimov, Thin Solid Films 6 (1970) 129.
[353] R.L. Stamps, R.E. Camley, R.J. Hicken, J. Appl. Phys. 81 (1997) 4485.
[354] R.L. Stamps, R.E. Camley, R.J. Hicken, Phys. Rev. B 54 (1996) 4159.
[355] H. Suhl, I.K. Schuller, Phys. Rev. B 58 (1998) 158.
[356] H. Hasegawa, F. Herman, Phys. Rev. B 38 (1988) 4863.
[357] P. Lambin, F. Herman, Phys. Rev. B 30 (1984) 6903.
[358] H. Hasegawa, F. Herman, Physica B 149 (1988) 175.
[359] A.P. Malozemoff, Phys. Rev. B 35 (1987) 3679.
[360] A.P. Malozemoff, Phys. Rev. B 37 (1988) 7673.
[361] A.P. Malozemoff, J. Appl. Phys. 63 (1988) 3874.
[362] N.C. Koon, Phys. Rev. Lett. 78 (1997) 4865.
[363] D. Lederman, C.A. Ramos, V. Jaccarino, J.L. Cardy, Phys. Rev. B 48 (1993) 8365.
[364] J. Nogués, D. Lederman, B.A. Gurney, I.K. Schuller, 1998, unpublished.